Study on the Establishment of a Glioblastoma Stem Cell Model and the Drug Delivery Targeting Glioblastoma Stem Cells

MARCH, 2018

HAFIZAH BINTI MAHMUD

Graduate School of

Natural Science and Technology

(Doctor's Course)

OKAYAMA UNIVERSITY

Study on the Establishment of a Glioblastoma Stem Cell Model and the Drug Delivery Targeting Glioblastoma Stem Cells

A dissertation submitted by **Hafizah Binti Mahmud** in partial fulfilment of the requirements for the Doctor of Philosophy in Engineering in the Graduate School of Natural Science and Technology, Okayama University, Japan.

March, 2018,

To my late father, *Mahmud bin A. Rahman* who was the true fighter of Kidney cancer (Renal Carcinoma) and never ever give up. Your strength becoming my inspiration

To my beloved husband, *Dr. Hj Mohd Aliff Afira* bin Sani who always gives me positive vibes and motivation

To my mother, *Rosmini binti A. Hamid* for who always gives endless love and blessings

To my *families* for their encouragements and support

ACKNOWLEDGEMENT

In the name of Allah, The Most Compassionate and The Most Benevolence who bestowed me the enlighten, the truth, the knowledge and with regards to Prophet Muhammad S.A.W for the guidance to the straight path. I thank to Allah for giving me the strength in completing this thesis. May Allah bless me with the ability to continue the good deeds to the community in this field.

Firstly, I would like to express my sincere gratitude and great appreciation to Prof Dr. Masaharu Seno because willing to accept me to be one of his student. His fatherly advice, guidance, encouragement and personality had inspired me to perform my work ability. He has nurtured me and weaned me to this peak of accomplishment. He genuinely deserves much of my gratefulness for his useful comments and contributions in revising my manuscript.

I would like to express the deepest appreciation to Dr. Tomonari Kasai, who has attitude and substance of a genius; he continually and convincingly conveyed a spirit of adventure regarding research. Without his guidance and persistent help, this achievement would not have been possible.

I additional extend my great thank to Associate Professor Dr. Hiroshi Murakami, Associate Professor Dr. Akufumi Mizutani, Dr Arun Vaidnayath, Dr Akimasa seno, Dr. Junko Matsuda, Dr Maram Hussein Zaky Zahra, Mrs Mami Asakura, Mrs Kaoru Furuse

and Mr Nobue Mukai for their kindly help, motivation and valuable idea throughout my study.

To Professor Takashi Ohtsuki and Professor Hiroshi Tokumitsu, they genuinely deserve much of my gratefulness for their useful comments and kindly reviewing my thesis.

Special thank should go to Aprilliana Cahya Khyraini, Aung Ko Ko Oo, Juan Du, Anna Sanchez Calle and Neha Nair for their guidance, help, encouragement and supports. My acknowledgement also goes to all the students from the Nano-biotechnology laboratory for their valuable suggestion and their friendliness giving me a wonderful memory of my doctoral course. Without them, this thesis would not have been the same as presented here.

I would like to convey my deepest thank to my families in Malaysia, especially my mother (Rosmini binti A. Hamid) and my parent- in law (Hj Sani Ithnin and Hjh Artini Dayat for their constant prayer, love and care for my success. Special appreciation to my husband, Dr. Hj Mohd Aliff Afira , the one whom have persistently given me strength, motivation, encouragements when needed, and constant prayer throughout my study. I would never have made this far without their support and love.

I also would like to thank my main sponsor: Majlis Amanah Rakyat (MARA) for the opportunity given in pursuant of this PhD study, Thank you.

CONTENTS

ABSTRACT OF THESIS

Glioblastoma is one of the most aggressive and invasive cancer with high mortality rates and poses several hurdles in the efficient chemotherapeutic intervention. Like other cancers, glioma also harbors cancer stem cells (CSCs), which are self-renewable and multipotent cells initiating the cancer incidence and exhibiting chemotherapeutic resistance and cancer recurrence. Previous study with our platform of microarray showed that CD44 is overexpressed in all glioma cancer cell lines analyzed but little expressed in the normal adult brain and fetal brain. CD44 is a multifunctional transmembrane glycoprotein which is considered as a marker specific to CSCs in various cancers. Since the principal ligand of CD44 is hyaluronan acid (HA), which is a major component of extracellular matrices, CSC population was thought to be condensed by exploiting HA affinity toward CD44.

In this study, U251MG cells were cultured under non-adherent condition in the presence of high molecular weight of hyaluronic acid (HA). The HA dependent spheroid forming population was then condensed and transplanted subcutaneously into Balb/c nude mouse. The primary cells excised from the resultant tumor were named as U251MG-P1

cells, which have been confirmed to express CD44 along with principal pluripotency genes, OCT3/4, SOX2, KLF4 and Nanog. U251MG-P1 cells were further characterized as CSC. After confirming the tumorigenicity of U251MG-P1 cells, we concluded that the U251MG-P1 was well established to provide a xenograft model of glioblastoma stem cells in nude mice.

Then this model was considered suitable to develop a drug delivery system targeting CSCs since U251MG-P1 cells exhibited tumor-initiating capacity while retaining the glioblastoma traits. Evaluating the sensitivity to anti-cancer agents, we found U251MG-P1 cells were sensitive to doxorubicin with IC50 at 200 nM. Although doxorubicin has serious side-effects, establishment of an efficient therapy targeting undifferentiated glioblastoma cell population is necessary. We previously designed a chlorotoxin peptide fused to human IgG Fc region without hinge sequence (M-CTX-Fc), which exhibited a stronger growth inhibitory effect on the glioblastoma cell line A172 than an original chlorotoxin peptide. Combining these results together, we designed M-CTX-Fc conjugated liposomes encapsulating doxorubicin and used U251MG-P1 cells as the target model in this study. The liposome modified with M-CTX-Fc was designed with a diameter of approximately 100–150 nm and showed high encapsulation efficiency, adequate loading capacity of anticancer drug, enhanced antitumor effects, demonstrating increasing uptake into the cells *in vitro*; M-CTX-Fc-L-Dox shows great promise in its ability to suppress tumor growth *in vivo* and it could serve as a template for targeted delivery of other therapeutics.

CHAPTER 1

GENERAL INTRODUCTION

1.0 Introducing Glioblastoma and Glioblastoma Stem cells.

The word “glioma” arise from glial cells. It is a type of tumor that originally from brain or spine. Glioma are categorized according to the specific type of cells from which its originate and degree of malignancy. World Health Organization (WHO) has been assigned glioma as glioblastoma (grade IV) , astrocytoma (grade I-III), oligodendro-glioma (grade II and III) , and mixed glioma (grade II and III) [1]. Grade I and II gliomas are clinically benign or semi benign with long -term survival while grade III and IV are malignant and lethal within several years. Among them, Glioblastoma multiforme (GBM) is the most aggressive and happened frequently to adult from ages 45-55 and predominance in males. The main standard care for patients with GBM consists of maximal surgical resection, radiotherapy and adjuvant chemotherapy with temozolomide [2]. Although extensive efforts have been done, most malignant glioma often relapse after treatments because of their normally diffuse infiltration into the surrounding brain.

1.1 Glioblastoma biomarkers

Tumor or cancer biomarker normally consist of wide variety of objects, including DNA, mRNA, secreted proteins, cell surface receptor, transcription factors, and metabolites, or processes such as apoptosis, angiogenesis or proliferation. They were produce either by the tumor itself or by other tissues or cells, in response to the presence of tumors or other associated in response to the presence of tumors or other associated irritation, like inflammation [3]. By identify the biomarker of cancer will give several

advantages such as can help doctors to profile the cancer predisposition, to give clue of cancerous stages, early diagnosis and prognosis after treatment and decide which drugs and what does it might be most effective to the patients with tumors.

1.1.1 Glial Fibrillary Acidic Protein (GFAP)

The common marker associated with glioma is glial fibrillary acidic protein (GFAP). It is a member of the cytoskeletal protein family and is widely detected in astrooglial cells and neural stem cells [4] . The serum GFAP levels of patients diagnosed with glioblastoma multiforme was significantly higher than those of patients with WHO grde II or III astrocytomas or of patients with brain metastases [5]. However, GFAP does not provide a better staining for distinguishing histologic subtypes of high grade glioma by immunohistochemistry [6]

1.1.2 Human cartilage glycoprotein-39 (YKL-40 or CHI3L1)

A secreted human cartilage glycoprotein -39 (YKL-40 or CHI3L1) also known as diagnostic markers for glioma. High level of YKL-40 also associated as a serum marker for several numbers of cancers including breast [7] , colorectal [8] and ovarian cancer [9]. Although it is often over-expressed in epithelial cancers, previous study has been suggested that YKL-40 is a marker associated with poorer clinical outcomes and a genetically defined histological subgroup of high grades gliomas. It is reporter having stronger marker for immunohistochemistry, provided a better class distinction compared

to GFAP marker. Alternatively, the combination of YKL-40 and GFAP will enhanced the diagnostic accuracy [6]. Moreover, the YKL-40 was also implicated as an important marker of radiation therapeutic response and genetic subtype in glioblastomas [10]. In the later year, except for YKL-40, matrix metalloproteinase-9 (MMP-9) protein was also highly differentially expressed in malignant gliomas. ELISA analysis from serum samples from patients with gliomas indicated that the both biomarker correlated with the patient's radiographic status and survival. Therefore, YKL-40 and MMP-9 may be used as a biomarker in glioma patients [11].

1.2 Glioblastoma Stem Cells

1.2.1 Concept of cancer stem cells

It is well believed that cancer tissues are heterogenous. It composed of various types of cells with different morphology and clinical phenotypes. This different has been explained by the stochastic clonal evolution model [12]. According to this model, all tumor cells should have low but inheritable ability to form tumor. However, another concept (hierarchy model) has been proposed, which shows that only a rare stem cell population called as cancer stem cells (CSC) has high ability to proliferate [13]. Similar characteristic with to normal stem cells, CSC having high ability to self-renew and

differentiate into multiple type of progenies. Contrarily with normal stem cells, CSCs can proliferate uncontrollably to propagate tumor cells.

Stochastic clonal evolution model; According to this model, tumor initiation occurs in the individual cells receiving multiple mutations, and cells having an advantageous mutation of growth can clonally proliferate and selectively occupy an entire tumor. During tumor progression, genetic instability yields the additional mutations by chance, resulting in a diversity of genome and cell characteristics, such as being invasive, metastatic and therapy-resistant. The adaptation to surrounding microenvironment is also a determinant of the selection. Standing on this concept, all the tumor cells should have low but inheritable ability to form tumors, therefore, the rational targets for cancer therapy is most or all of tumor cells. (Figure 1)

Hierarchy model; Cells may acquire various genetic and epigenetic mutations that confer stem-like characteristics, and divide to produce its identical copy (self-renewal) and progenies terminally growth-arrested (differentiation). Such a hierarchy in a stem cell division manner results in cellular diversity of a rare stem cell and most of multiple types of progenies (Figure 1)

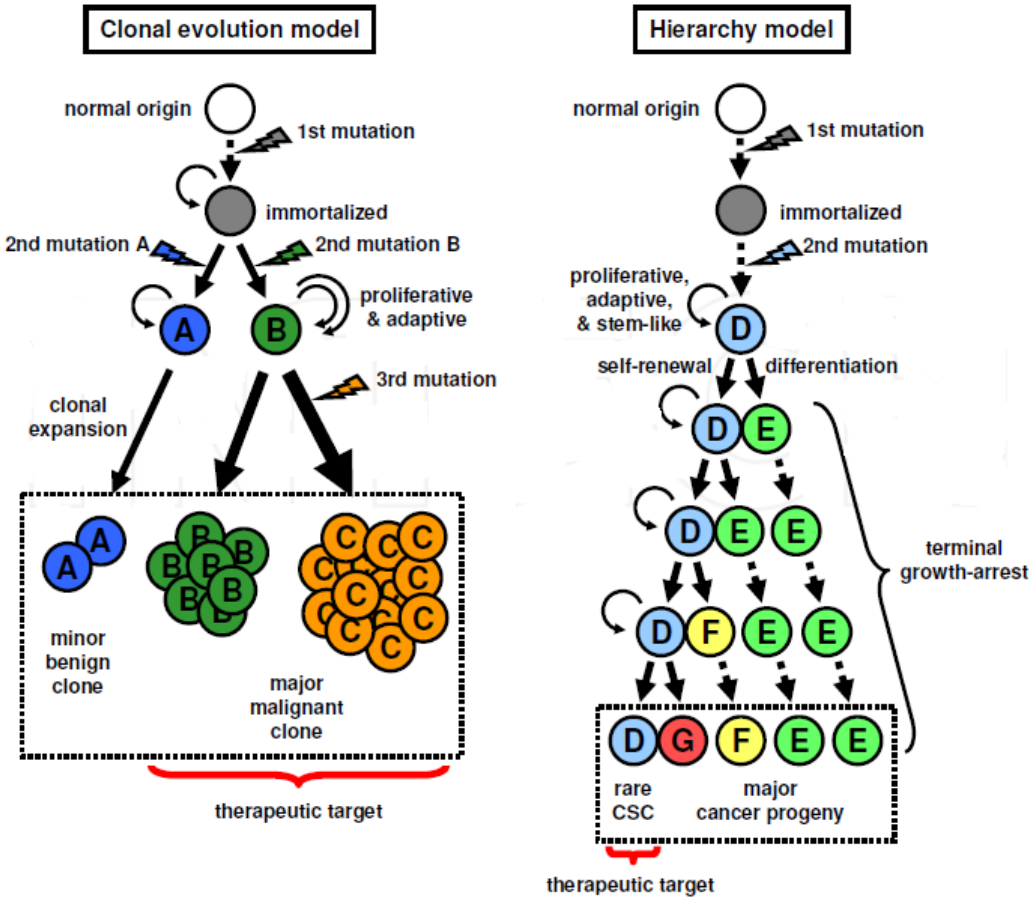

Figure 1: Clonal evolution model and hierarchy model (Tabu et al.,2011).

1.2.2 Methods to isolate cancer stem cells

1.2.2.1 Sphere formation assay

In the first place, the sphere formation assay was first developed to characterize the behaviour of neural stem cells [14]. Cells were cultured into low attachment dish in

serum free media supplemented with mitogen (epidermal growth factor and fibroblast growth factor for neural stem cells). In those condition, only cancer stem cell will survive by forming floating spherical cell clusters while differentiated cells will be died. Therefore, the number and diameter of spheres are thought to reflect the frequency of stem cells and mitotic activity of a single stem cell within the examined population, respectively. When a 1st sphere is picked up, re-dissociated into single cells, and re-cultured, the generated secondary spheres indicating the sustained self-renewal potential of a true stem cell. However, sphere formation assay has several limition for isolation of some types of CSCs in which condition of sphere assay for normal stem cells is unestablished, it is uncertain if they have significance for stem cell activity in the tissues.

1.2.2.2 Hoechst 33342 dye effluxing side population (SP)

Hoechst 33342 is a fluorescent dye and also one of dye transport-based assay. The dye becomes fluorescent after entering the cell and binds to the AT-rich regions of DNA. In most cases , stem cells are not stained due to high expression of ABC transporter family genes to efflux this dye. Human fetal neural stem/progenitor cells express high levels of multidrug resistance 1 (MDR1, also known as ABCB1, P-gp) gene and ATP-binding cassette sub-family G member 2 (ABCG2, also known as Bcrp), and these transporters have important roles in normal physiology on the active efflux of xenobiotics from cell body, protecting cells from cytotoxic agents.

References

1. McCarthy, B.J., et al., *Assessment of type of allergy and antihistamine use in the development of glioma.* Cancer epidemiology, biomarkers & prevention : a publication of the American Association for Cancer Research, cosponsored by the American Society of Preventive Oncology, 2011. **20**(2): p. 370-378.
2. Sathornsumetee, S., et al., *Molecularly targeted therapy for malignant glioma.* Cancer, 2007. **110**(1): p. 13-24.
3. Kulasingam, V. and E.P. Diamandis, *Strategies for discovering novel cancer biomarkers through utilization of emerging technologies.* Nature Clinical Practice Oncology, 2008. **5**: p. 588.
4. Yang, X.-y., et al., *Hyaluronic acid-coated nanostructured lipid carriers for targeting paclitaxel to cancer.* Cancer Letters, 2013. **334**(2): p. 338-345.
5. Jung, C.S., et al., *Serum GFAP is a diagnostic marker for glioblastoma multiforme.* Brain, 2007. **130**(12): p. 3336-3341.
6. Nutt, C.L., et al., *YKL-40 Is a Differential Diagnostic Marker for Histologic Subtypes of High-Grade Gliomas.* Clinical Cancer Research, 2005. **11**(6): p. 2258-2264.
7. Jensen, B.V., J.S. Johansen, and P.A. Price, *High Levels of Serum HER-2/neu and YKL-40 Independently Reflect Aggressiveness of Metastatic Breast Cancer.* Clinical Cancer Research, 2003. **9**(12): p. 4423-4434.

8. Cintin, C., et al., *Serum YKL-40 and colorectal cancer.* British Journal of Cancer, 1999. **79**(9-10): p. 1494-1499.

9. Dehn, H., et al., *Plasma YKL-40, as a prognostic tumor marker in recurrent ovarian cancer.* Acta Obstetricia et Gynecologica Scandinavica, 2003. **82**(3): p. 287-293.

10. Pelloski, C.E., et al., *YKL-40 Expression is Associated with Poorer Response to Radiation and Shorter Overall Survival in Glioblastoma.* Clinical Cancer Research, 2005. **11**(9): p. 3326-3334.

11. Hormigo, A., et al., *YKL-40 and Matrix Metalloproteinase-9 as Potential Serum Biomarkers for Patients with High-Grade Gliomas.* Clinical Cancer Research, 2006. **12**(19): p. 5698-5704.

12. Nowell, P., *The clonal evolution of tumor cell populations.* Science, 1976. **194**(4260): p. 23-28.

13. Jordan , C.T., M.L. Guzman , and M. Noble *Cancer Stem Cells.* New England Journal of Medicine, 2006. **355**(12): p. 1253-1261.

14. Reynolds, B. and S. Weiss, *Generation of neurons and astrocytes from isolated cells of the adult mammalian central nervous system.* Science, 1992. **255**(5052): p. 1707-1710.

Chapter 2

Hyaluronic Acid Mediated Enrichment of CD44 Expressing Glioblastoma Stem Cells in U251MG Xenograft Mouse Model

LIST OF ABBREVIATIONS AND ACRONYMS

CSC	Cancer stem cell
cDNA	Complementary DNA
GBM	Glioblastoma multiforme
HA	Hyaluronic acid
HCI	Hydrochloric acid
HBSS	Hank`s Balance Stock Solution
h	Hours
EDTA	Ethylenediamineteraacetic acid
EMT	Epithelial Mesenchymal Transition
ECM	Extracellular Matrix
ES cells	Embryonic Stem Cell
FBS	Fetal Bovine Serum
RNA	Ribonucleic acid
qRT-PCR	quantitative Reverse Transcription Polymerase Chain Reaction
mm^3	Cubic milimeter
mL	Mililiter
min	Minutes

OCT	Optimum cutting temperature
rpm	Revolutions per minutes
µg	Microgram
µm	Micrometer

LIST OF TABLE

LIST OF FIGURES

Abstract

Glioblastoma is one of the most aggresive cancer with high mortality rates and poses several hurdles in the efficient chemotherapeutic intervention. Similar to other cancers, glioma also haarbors CSCs, that are self renewable, multipotent cells, which innitiate the cancer incidence, chemotherapeutic resistance and cancer recurrence. The microenviroment regulation in the brain tumor and metastasis involves the cooperative interaction between HA and CD44. CD44, being a multifaceted transmembrane glycoprotein by itself, or in combinatiom with several other cell surface receptors, has been used as a marker for CSC isolation. We established both adherent and non adherent culture of U251MG cells by treating with high molecular weight HA. Further these cells were transplanted subcutenously in Balb/c mouse for the generation of the xenograft model for the cancer stem cell. The tumor was further characterized for the establishment of the working model for molecular targeting studies of cancer stem cells. Here we showed the enrichment of the CD44 expressing population of glioblastoma cells by induction with hyaluronic acid. The non-adherent culture spheroids of U251MG cells showed up regulation in the CD44 expression along with aberrant activation of principal pluripotency genes OCT3/4, SOX2, KLF4 and Nanog. Using the HA-treated spheroid, we established an experimental xenograft mouse model with high angiogenesis enhanced tumor-initiating capacity while retaining the glioblastoma traits.We characterized a mouse model of

U251MG cells which could be a promising model system to study the molecular targeting approaches against CSCs in glioblastoma.

1.0 Introduction

Glioblastoma multiforme is the one of the most malignant cancer affecting the brain making them one of the incurable cancers with a survival rate of 5%. Several studies have shed light on the cytogenetic, molecular and epigenetics alterations during its incidence and have characterized the tumor to its molecular level [1]. Histopathological attributes have helped in the classifying gliomas into two broad lineages: astrocytoma and ologodendroma and four grades (I-IV) of which the grade I and II corresponds to the low-grade glioma and III and IV correspond to the high- grade gliomas [2]. Glioblastoma cells are non-invasive outside the brain partly because of the effective blood brain barrier and the multitude of the complex microenviroment which it requires for the metastasis [3]. With the progression of the tumor metastatic cells uses the neovascularization for the spread of cancer and the blood- brain barrier changes to a blood-tumor barrier. Considering the microenvironment in the brain and its relative complexity in targeting the blood-tumor barrier are less receptive to chemotherapeutic intervention [4]. Glioma, like other cancers, are highly heterogenous and shows hierarchy in their progression with the apex being the Cancer Stem Cells (CSCs) which repopulates the whole of the tumor. The CSCs are believed to be the primordial reason for the recurrence and reinstatement of the tumor after chemotherapeutic intervention and surgery as they are radiation and chemotherapeutics resistant [5]. The perpetual self- renewability of the CSC is a complex process, which is mediated by the cellular and soluble attributes of the tumor

microenviroment which includes the extracellular matrix, mesenchymal cells, endothelial cells and secretory molecules comprising cytokines and growth factor. The microenviroments surrounding the CSCs are termed as niche which modulates the cellular fate of the CSC [5-7].

CD44 is a multifunctional transmembrane glycoprotein which is a commonly used marker for isolating the CSCs from various cancers and mediating cell-cell and cell-matrix interactions furthering the malignancy and cancer dissemination. CD44 is typically associated with CD24, CD133, and CD34 for the enrichment of the various cancers.

Hyaluronic Acid (HA) biosynthesis in the tumor microenvironment has been shown to increase the cancer aggressiveness and poor clinical outcome affecting the overall survival rate of the patients [8, 9]. Previous study with our platform of microarray showed that CD44 is overexpressed in all glioma cancer cell lines analyzed but little expressed in the normal adult brain and fetal brain [10]. In breast cancer cells, HA overexpression drives EMT which is one of the key aspects of the CSC generation and propagation [11]. Over recent years, CD44 along with other cell surface markers like CD133, CD90, CD24, ALDH, Nestin, EpCAM, and CD34 are also associated with CSC isolation and enrichment in various tumors [12]. In addition to its naturally occurring ligand, CD44 interacts with several ECM molecules including fibronectin galectin-8, laminin, fibrinogen, chondroitin sulfate and osteopontin [13, 14]. Since the principal ligand of CD44 is hyaluronan acid (HA), which is a major component of extracellular

matrices, CSC population was thought to be condensed by exploiting HA affinity toward CD44.

In this study, U251MG and A172 cells were cultured under non-adherent condition in the presence of high molecular weight of hyaluronic acid (HA). The HA dependent spheroid forming population was then condensed and transplanted subcutaneously into Balb/c nude mouse. The primary cells excised from the resultant tumor were further characterized as CSC. **(Figure 1)**

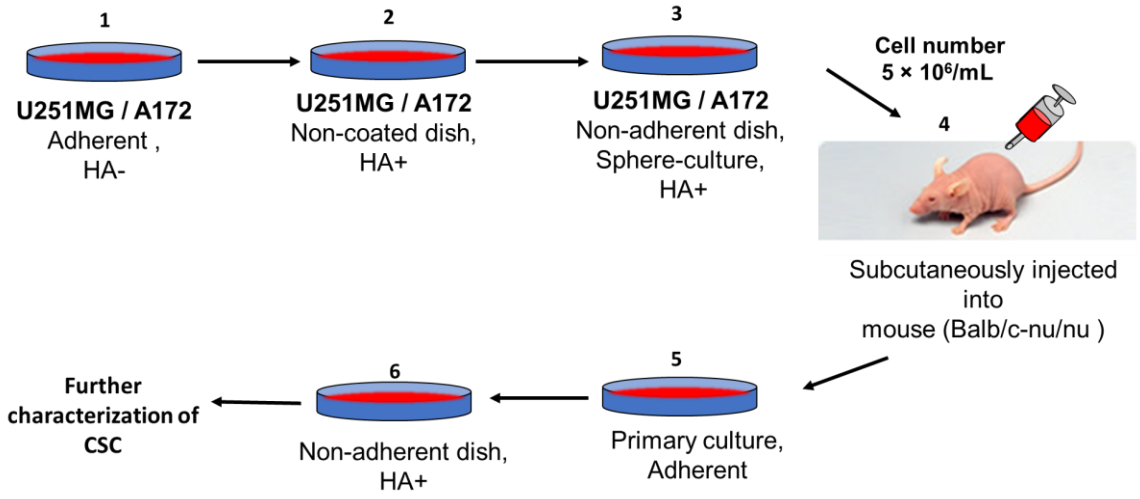

Figure 1: Scheme of glioma stem cell establishment mediated by HA. 1) Glioma cells line (U251MG / A172) were cultured in adherent plate until confluent. 2) Cell then transferred into non-coated dish supplemented with HA 3) 1x 10^4 / mL of cells were transferred into non-adherent dish for sphere culture with addition of HA 4) The resulting spheroids were

injected into nude mouse, where they generated malignant tumor. 5) The primary cells excised from the resultant tumor were culture in adherent dish until confluent 6) Prior to further characterized as CSC, cells were transferred into non- adherent dish to form spheres and were condensed with HA.

2.0 Materials and Methods

2.1 Cell culture

U251MG and A172 were cultured as per protocol decribed elsewhere [10].For primary cultures, mouse xenografts were cut into small pieces of 1 mm^3 in HBSS. The tumor were further washed three times and were transferred to a 15-ml conical tube with 0.25% trypsin (3-4 fold) for 30 min at 37°C and were stopped by the addition of media containing FBS. The cell suspension was spun down at 800 rpm for 10 min. The cell pellet was washed with HBSS and was suspended in complete media and seeded into a dish at a density of 5-6 $\times 10^5$ cell /mL. Cells were passaged every 3 days and cells morphology was observed and photographed using Olympus IX81(Olympus, Japan) microscope equipped with a light flourescence device.

2.2 Sphere Formation and HA treatments

For the sphere formation assay, the cell number were adjusted to 1×10^4 /mL and were cultured in ultra-low attachment dishes in the media devoid of FBS and containing

Insulin/ Transferrin/ Selenium-X (ITS-X) and 100 µg/mL HA. The media without the supplementation of HA were included as a control. The cells were continued culturing for another 4 days and the spheres were distrupted to form secondary spheres for an additional culturing for 2 days. Spheres reaching 100 µm were considered as self-renewing and were used for all the analysis.

2.3 Experimentals animal

The nude mice (Balb/c-nu/nu, female, 4 weeks old) were obtained from Charles River , Japan. For all the transplantation studies, 1×10^6 cells were suspended in 200 µL in complete media and were injected subcutenously . Size and volume measurement were done every 3-4 days with the following formula $0.5\times \text{width}^2\times\text{length}$, in which width is the smallest diameter and length is the longest diameter. After 5 weeks, tumors were extracted and separated in 4 equal parts that were used for the primary cell culture and histological analysis. The animals were maintained in dedicated animal facility in Okayama University . All the animal experiments conducted were carefully designed and executed as per general gudelines stipulated by the ethics committee of Okayama University.

2.4 RNA Extraction and RT-qPCR

Total RNA was isolated by RNeasy Mini Kit (QIAGEN, Germany) and treated with DNase Amplification Grade (Invitrogen, CA). cDNA synthesis was performed using SuperScript III First strand kit (Invitrogen, CA). RT-qPCR was performed with Cycler 480 SYBR Green I Master mix (Roche, Switzerland. The primers used for detect the cDNAs of interest are tabulated in **Table 1**.

Table 1 : Primer sequences used in RT-qPCR analysis.

Gene	Sequence (5'-3')	
Nanog	F	CAGCCCCGATTCTTCCACCAGTCCC
	R	CGGAAGATTCCCAGTCGGGTTCACC
OCT3/4	F	GACAGGGGGAGGGGAGGAGCTAGG
	R	CTTCCCTCCAACCAGTTGCCCCAAAC
Sox2	F	GGGAAATGGGAGGGGTGCAAAAGAGG
	R	TTGCGTGAGTGTGGATGGGATTGGTG
KLF4	F	ACGATCGTGGCCCCGGAAAAGGACC
	R	TGATTGTAGTGCTTTCTGGCTGGGCTCC
CD44s	F	AAGGAGCAGCACTTCAGGAG
	R	GGACCAGAGGTTGTGTTTGC
CD44v3	F	AAGGAGCAGCACTTCAGGAG
	R	GGTCCAGTCCTGGTTCTGTT

CD44v4	F	AAGGAGCAGCACTTCAGGAG
	R	GTGTGCTTCTGGGTTCCAGT
CD44v6	F	AAGGAGCAGCACTTCAGGAG
	R	CTGGGCTTGGTGTTGTCCTT
CD44v8	F	AAGGAGCAGCACTTCAGGAG
	R	TCTTCTTCCAAGCCTTCATGTG
CD44v10	F	AAGGAGCAGCACTTCAGGAG
	R	GATCCATGAGTGGTATGGGACC
CD44 v8-10	F	AAGGAGCAGCACTTCAGGAG
	R	GGGTGGAATGTGTCTTGGTCT
CD133	F	CGCGTGATTTCCCAGAAGATACT
	R	ATACCCCACCAGAGGCATCA
NFKB p105	F	CGGGAAAAAGAGCTAATCCGC
	R	GATGCATTGGGGGCTTTACTG
REL B	F	TGGATCCTGTGCTTTCCGAG
	R	ACACCACTGATATGTCCTCTTTCT
GAPDH	F	TGGTATCGTGGAAGGACTCA
	R	CCAGTAGAGGCAGGGATGAT

*F : Forward primer; R : Reversed Primer

2.5 Cell Lysis and Western Blotting

Total cell extracts were collected as follows : Cells were lysed in 300 uL of lysis buffer (10 mM Tris-HCI, pH 7.5, 5 mM EDTA, 150 mM NaCI, 1% Triton -X 100, 10% (v/v) glycerol) containing protease inhibitor cocktail for 30 min at 4°C. The lysate was then sonicated for 30 secs; 2 times and were collected for the subsequent analysis. Cell extracts isolated were then subsequently separated in polyacrylamide gels, transferred onto PVDF membrane and incubated with specific antibodies as indicated. Immunoreactivity was revealed by chemiluminescense as per the manufacturer`s instructionand measured using the Atto imaging system (Atto, Japan).

2.6 Immunohistochemistry and histological analysis

The tumor extracted from the animal were primarily fixed with paraformaldehyde for 24 h followed by paraffin embedding procedure for histochemical analysis. The fixed tissues was then thoroughly washed and were permeated with increasing concentration of sucrose. Tissue blocks were made with OCT reagent (Sakura-Finetek, Netherland) and were stored at-80°C until processing . The samples were fixed with absolute methanol for 10 min followed by blocking of the endogenous peroxidase with 3% H_2O_2 for 10 min. Using the Ellite anti-rabbit ABC vectastain kit (Vector Laboratories, USA), anti -CD-31 (1:100 , ab28364, Abcam, UK) and anti-CD133 (Novus Bio, USA), anti- LYVE-1

(Abcam,UK) antibodies were incubated for 2 hrs at room temperature. Immunoreactivity were detected by using DAB following the manufacturer`s recommendations. Images of the sections were processed with the FSX100 microscope (Olympus, Japan) for analysis and identification of the tumor type.

3.0 Results and Discussion

3.1 HA mediates enrichment of CD44 expressing population

High molecular weight HA stimulates the CD44 mediated clustering of breast cancer cells [15]. The CD44 binding to HA also has various outcomes based on the size of HA binding to CD44 such as pro-angiogenic and pro-inflammatory while nHA promoted anti-angiogenic and anti-inflammatory effects [16-18]. To assess the HA mediated enrichment of CD44, we cultured A172 and U251MG glioblastoma cells in both adherent and non-adherent conditions at a concentration of 100 µg/mL of HA. The cells in the adherent conditions without HA were bound to the plate while the spheroids formation could be seen with the non-adherent HA+ treated cells (**Figure 2A**). The increment in the spheroid formation was further confirmed with culturing the A172 and U251MG with (HA+) and without (HA-) the addition of HA in the culture medium (**Figure 2B).**

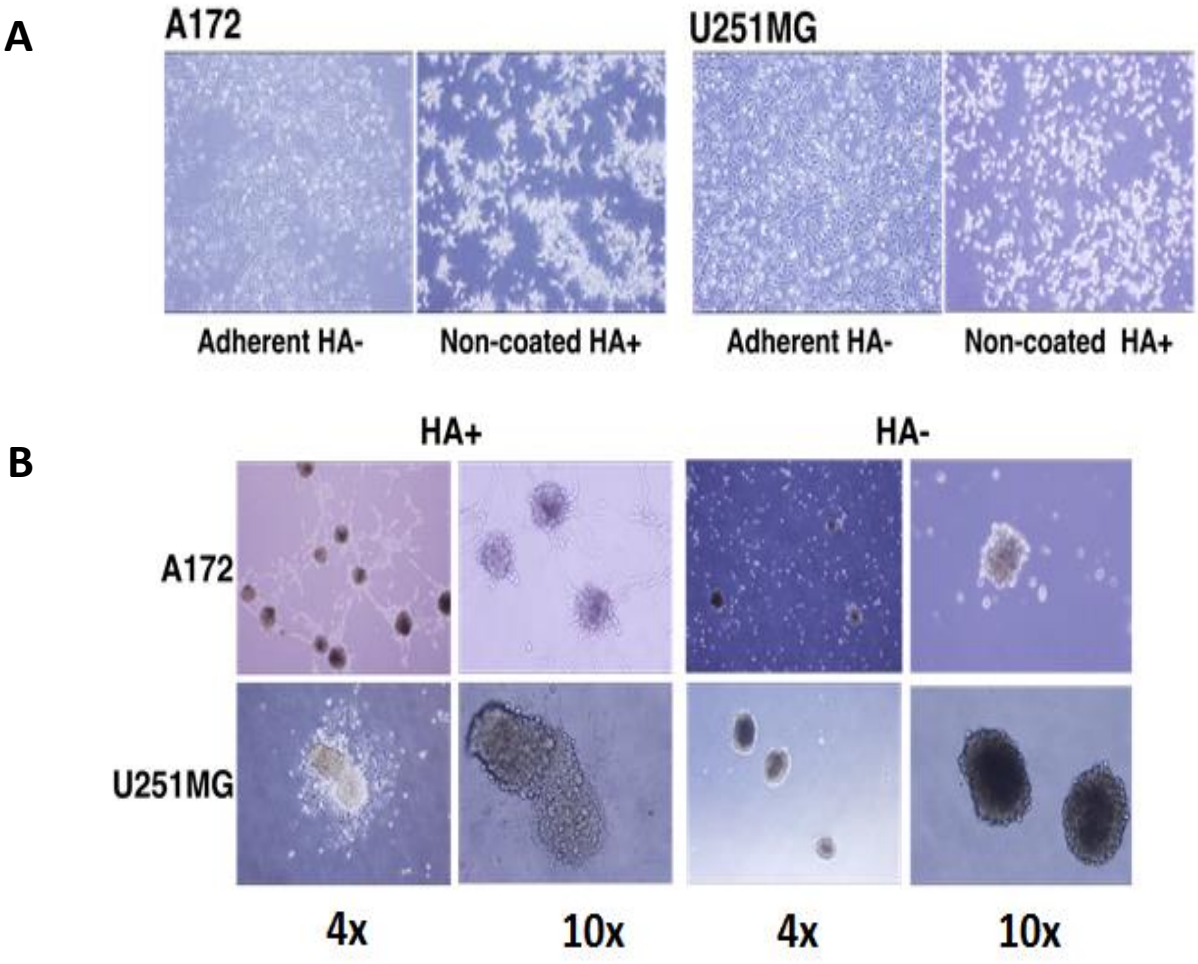

Figure 2: Induction of A172 and U251MG cells with HA. A) Cell morphology of A172 and U251MG cells on adherent and non-coated dish. B) Spheriod formation of A172 and U251MG cells in the presence or absence of HA for 2 weeks.

3.2 CD44 expression is upregulated by HA

We next checked the expression of CD44 in A172, U251MG by qRT-PCR. The expression analysis was done between the cell lines treated with HA+ and HA- and between the adherent culture and non-adherent culture. In U251MG and A172 cell lines the CD44 expression was up regulated 3 folds in non-adherent HA+ cells when compared with adherent HA- counterpart (**Figure 3A and 3B**). The gene expression was further checked in the protein expression level through immunoblots with the cells. The immunoblot results clearly show that the HA-treated cells express more CD44 when compared to non-treated samples (**Figure 3C**).

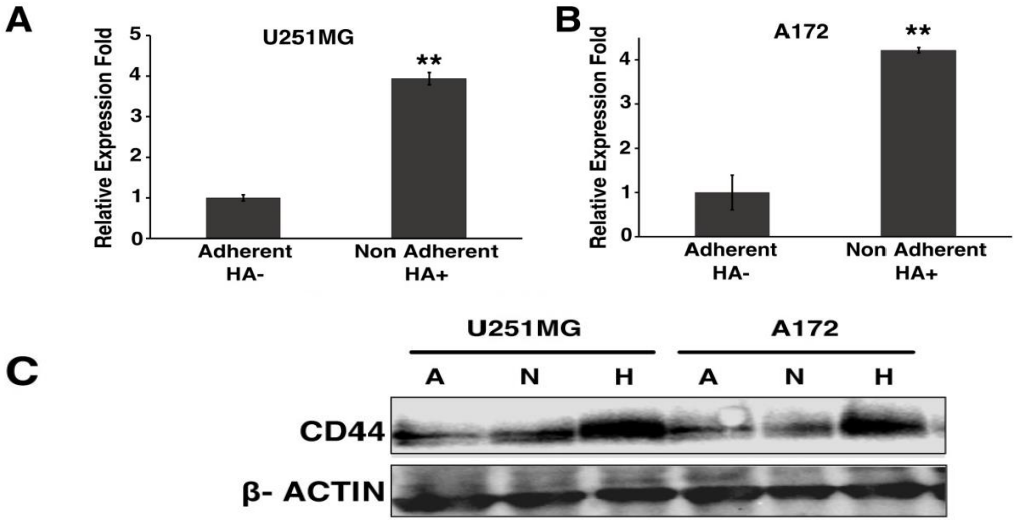

Figure 3 : Up regulation of CD44 expression in U251MG and A172. CD44 expression of adherent HA- and nonadherent HA+ treatment by qRT-PCR of (A) U251MG and (B)

A172. (C) Protein expression was further confirmed with the various treatment in A172 and U251MG cell; A: Adherent, N: Non-adherent, H: Non-adherent HA+ .

3.3 Generation of glioblastoma mouse model

Using the HA-induced CD44 up regulation, we developed a glioblastoma mouse CSC model. We injected the spheres cultured of A172 and U251MG in the presence of HA into the mouse subcutaneously. However, tumor is not form in mouse injected with spheres cultured of A172 possibly because it is non-tumorigenic in immunosuppressed mice. In mice injected with spheroids cultured of U251MG, the tumor incidence time was faster in the [19]treated spheres within 40 days when the adherent culture injected mouse showed no signs of tumor formation substantiating tumor-initiating population in the HA cultured spheroids. HA-treated spheroids generated tumors faster in the mouse by several folds when compared with the cultures of U251MG cells cultured without HA in adherent conditions. Thus, the CD44 induction with the non-adherent conditions is found to be the deciding factor for the reduced tumor latency in the mouse (**Figure 4A and B**).

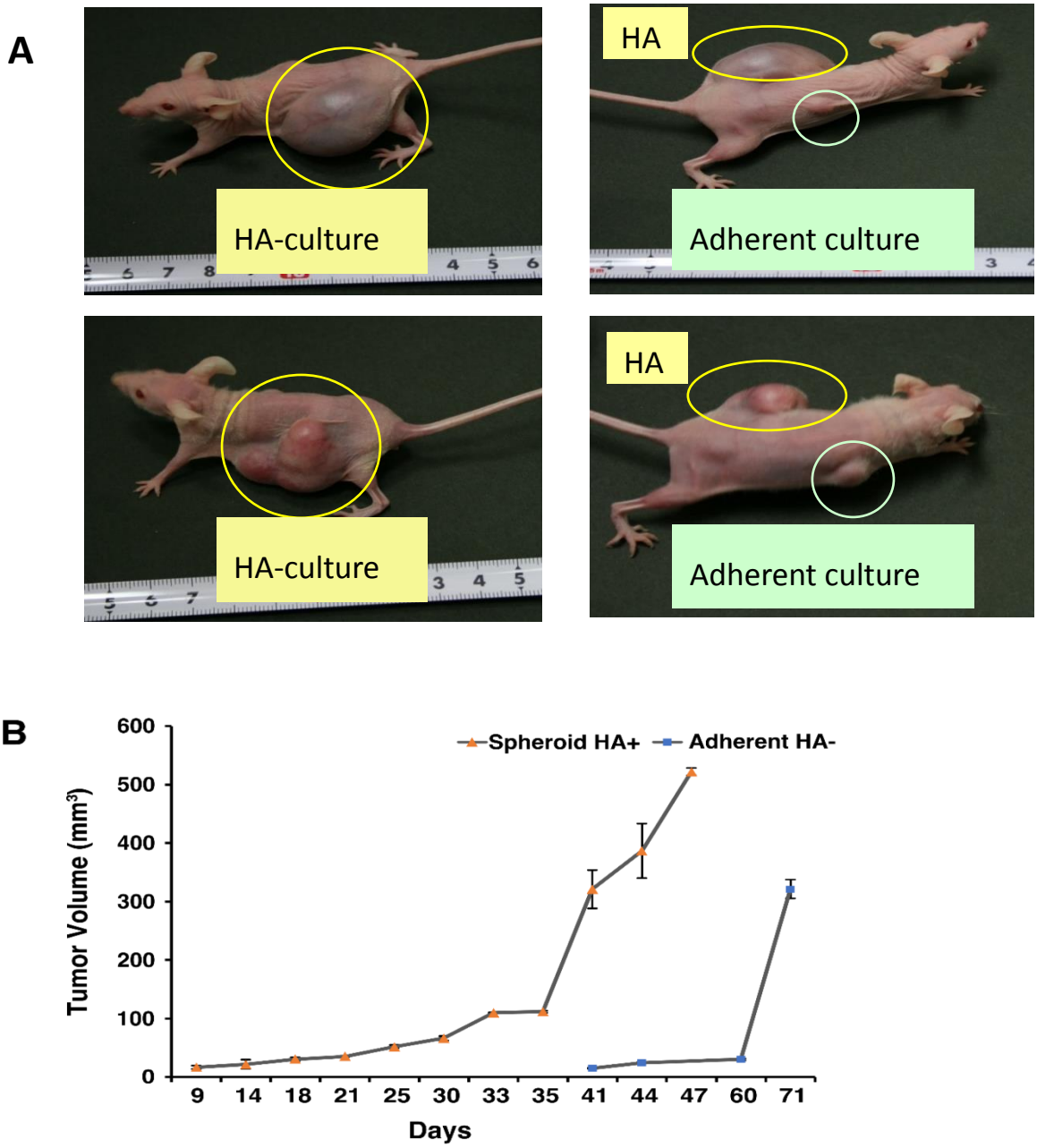

Figure 4 Characterization of mouse model of glioma . (A) Tumor formation in mouse with U251MG spheroids treated with HA and adherent culture of U251MG without the

HA treatment. (B) Tumor incidence rate with spheroid/HA+ and adherent/HA- cultures of U251MG cells; n=2.

3.4 Analyses of primary cells excised from the resultant tumor (U251MG-P1) compare with parental cell line (U251MG)

3.4.1 Enrichment of spheroid forming population mediated by HA

The primary cells excised from the tumor-bearing mouse were named as U251MG-P1. The U251MG-P1 showed enrichment of more spheroid forming population when compared with the parental cell line (**Figure 5A**). The increment in the spheroid formation was further confirmed with culturing the U251MG-P1with (HA+) and without (HA-) the addition of HA in the culture medium (**Figure 5B**). The sphere formation was enhanced in U251MG-P1 resembling the stem cell morphology, while the parental cell line showed loosely formed aggregates with more differentiated cells.

To test the self-renewal in the tumor spheroids generated by the treatment, we dissociated the cells to single cells suspension with collagenase treatment and were cultured for 2 weeks with HA in adherent conditions (**Figure 5C**). The cells retained the spheroid forming ability which resembles that of the CSCs. The presence of HA-CD44 interaction in the cells promotes the aggregation and the CD44 over expressing population should be the reason for the reconstitution of the spheroid formation. The spheroid

formation and the incidence time for the sphere formation were up regulated with the treatment of HA.

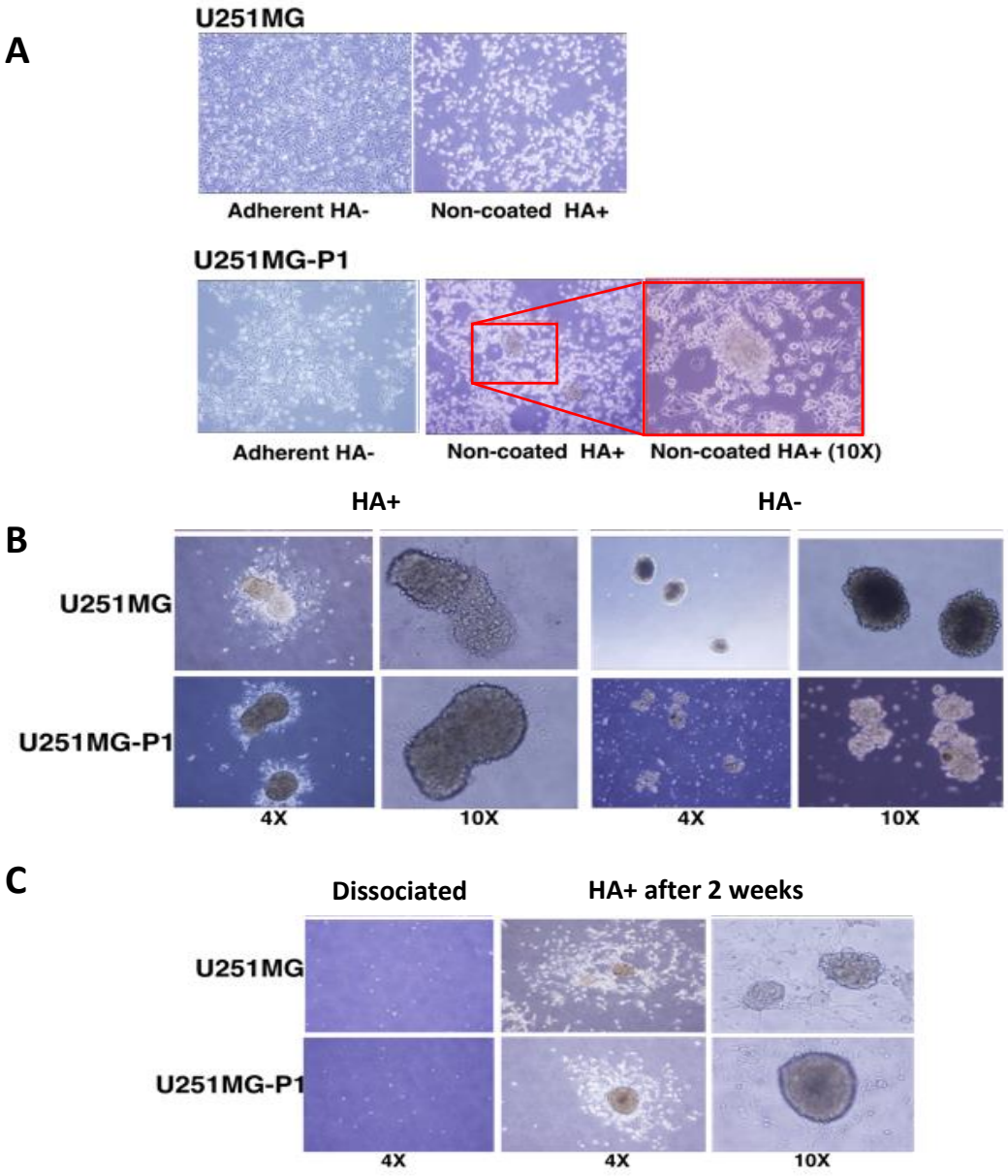

Figure 5 : Spheroid population in U251MG and U251MG-P1.A) Cell morphology of U251MG and U251MG-P1 on culture dish without HA and on non-coated dish with 100

μg/mL HA. Inset (red box) shows the magnified image of the spheroid formation of U251MG-P1 cells in non-coated dish with HA. B) Spheroid formation of U251MG and U251MG-P1 cells in the presence or absence of HA for 2 weeks. C) Cell morphologies of U251MG and U251MG-P1 after dissociation and culturing with HA for 2 weeks in adherent conditions.

3.4.2 CD44 gene expressing

We further compared the enrichment of the CD44 expression in the population of cells U251MG and U251MG-P1 in the adherent and spheroid conditions with and without the induction of HA The relative CD44 gene expression in U251MG and U251MG-P1 cells were assesed using RT-qPCR . Relative expression of CD44 in cell lines treated with HA was up-regulated 2 fold for both cell when compared with adherent HA- conditions. All results from these experiments proved that the CD44 expression is considerably up regulated by the treatment with HA there by the enrichment of the CD44 expressing population (**Figure. 6A**). We further analyzed the effect of CD44 isoform expression in U251MG and U251MP1cells. We found the expression of standard, V4, V8, V10 and V8-10 to be up-regulated in U251MG-P1 (**Figure. 6B**).

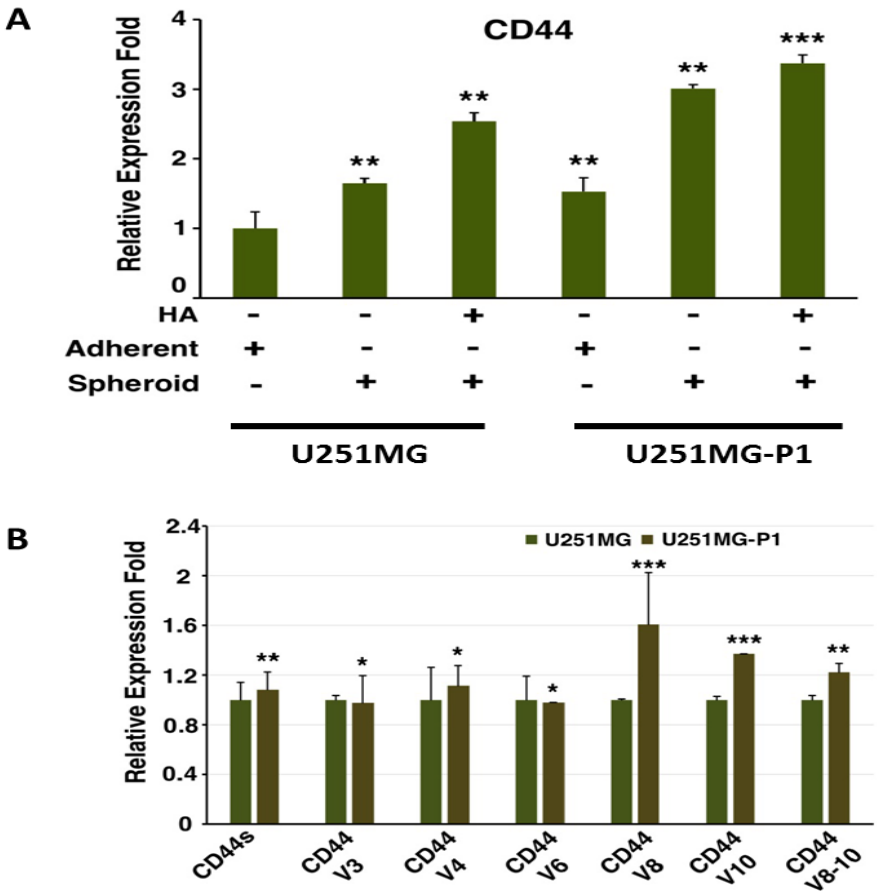

Figure 6 : Relative CD44 gene expression in U251MG and U251MG-P1.A) U21MG and U251MG-P1 cells were cultured under adherent and non-adherent condition with or without the supplementation of HA. RT-qPCR was performed and relative expression fold of CD44 was calculated. B)) Quantitative PCR analysis of the expression of CD44 isoforms in U251MG and U251MG-P1 cells in adherent conditions. The data depicted are generated from two independent experiments.

3.4.3 HA induces the expression of pluripotent genes

Aberrant activation of the pluripotent genes augments cancer initiation, progression, and chemotherapeutic resistance. These transcription factors are found to be over-expressed in several of the cancers and were used to identify cancer stem cell-like cells in glioblastoma [20]. HA-CD44 interaction was proved to activate Nanog which is principally involved in the stem cell maintenance and self-renewal in the ES cells [21-23]. The activation of CD44 through the PKCε phosphorylates Nanog, with or without the association of Stat3 regulates the expression of other pluripotent, tumorigenic and multidrug resistance genes [22]. Nanog has shown to regulate the expression of Sox2, Oct3/4, and Rex1, the prominent pluripotent transcription factors during ES cell pluripotency. To assess the activation of embryonic pluripotency genes, we performed the RT-qPCR for the various treatment of the cells in the conditions depicted in **Figure 7**. The cells treated with HA augments the expression of pluripotency genes suggesting the possible acquiring of stem cell characteristics (**Figure 7A**). Since Sox2 has been proved to be the principal pluripotency genes in the generation of CSC, we analyzed the expression further with immunoblots (**Figure 7B**).

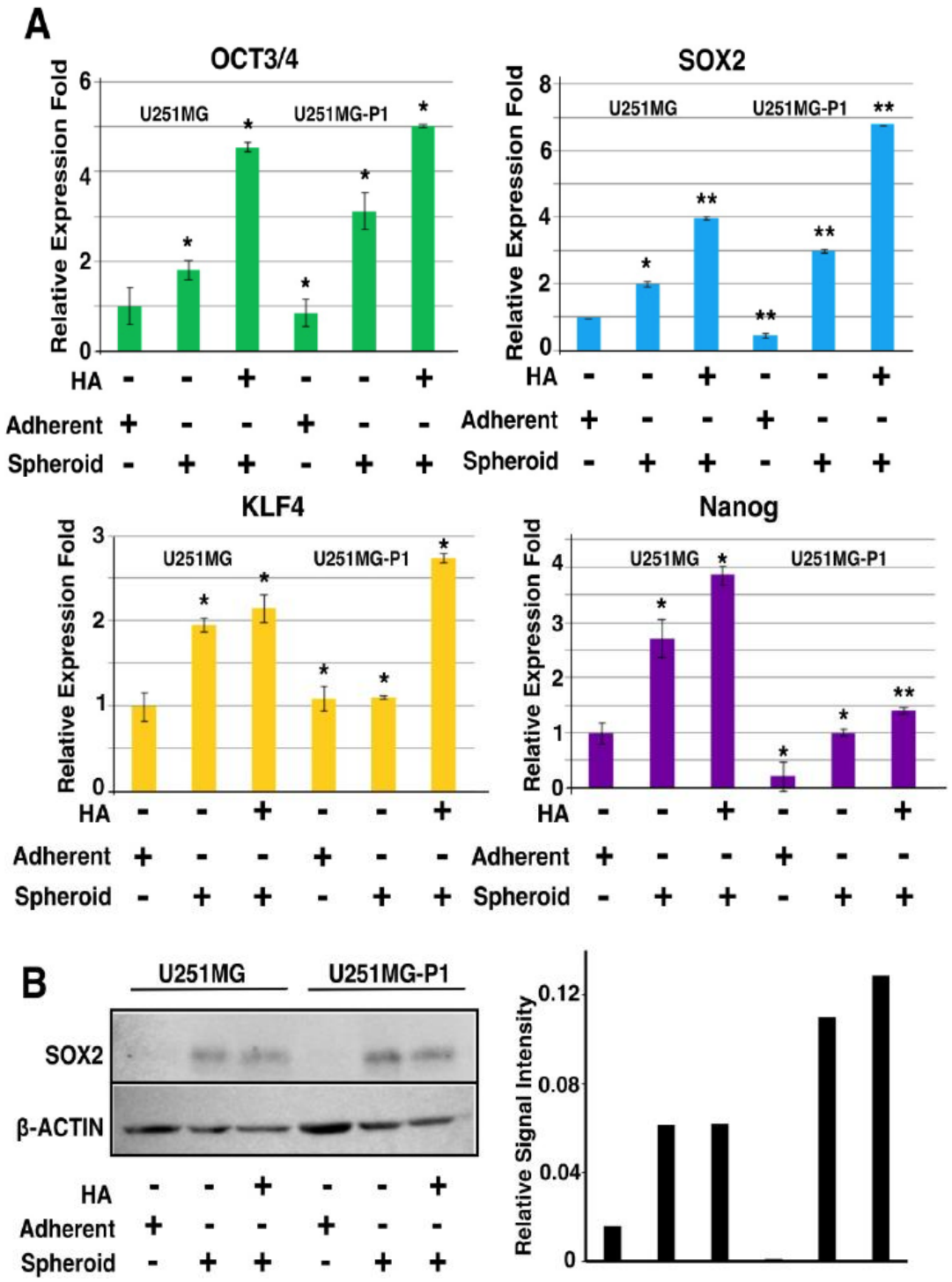

Figure 7: Expression of pluripotent genes in U251MG and U251MG-P1 cells. (A) Cells

were cultured with or without HA in adherent or nonadherent conditions, RT-qPCR analysis was performed with the primers for Sox2, Oct3/4, Klf4 and nanog. Error bar represents the mean SD of two independent experiments. Data are the mean of independent experiments and the p values were calculated by Tukey HSD analysis (*$p<0.05$, **$p<0.01$; n=3). (B) Cells cultured under the different conditions were lysed, separated on SDS-PAGE and were immunoblotted for Sox2 expression. The normalized relative band intensity was calculated from the blot and were plotted as a graph using ImageJ.

3.4.4 Activation of NFkB signalling in U251MG-P1 cells

Activation of inflammatory and angiogenic mediators in U251MG-P1 cells NFκB complex activates MMP-9 and several other genes which are key response elements in the tumorigenesis and stem cell maintenance through tumor microenvironment mediated inflammation and ECM signaling [24-26]. To test the activation of inflammatory mediators we checked the NFκB activation in the HA-treated spheroids. NFκB activation has been associated with the mesenchymal subtype of the glioma and is proved to provide radioresistance in cancer [27]. We found that the HA induces p50/105 activation in the U251MG-P1 cells consistent with the results got from the high-grade glioblastoma models. Further, we found that p65 is activated in both parental and U251MG-P1 cells. Based on these observations we then checked for the genes involved in the NFκB family by

quantitative PCR and we found that the NFKB1, which is essential for the translocation of the p50/65 complex into the nucleus for the gene regulation, was suppressed, and REL-B was found to be expressing in the U251MG-P1 cells showing the mesenchymal nature of the primary tumor cells (**Figure 8**).

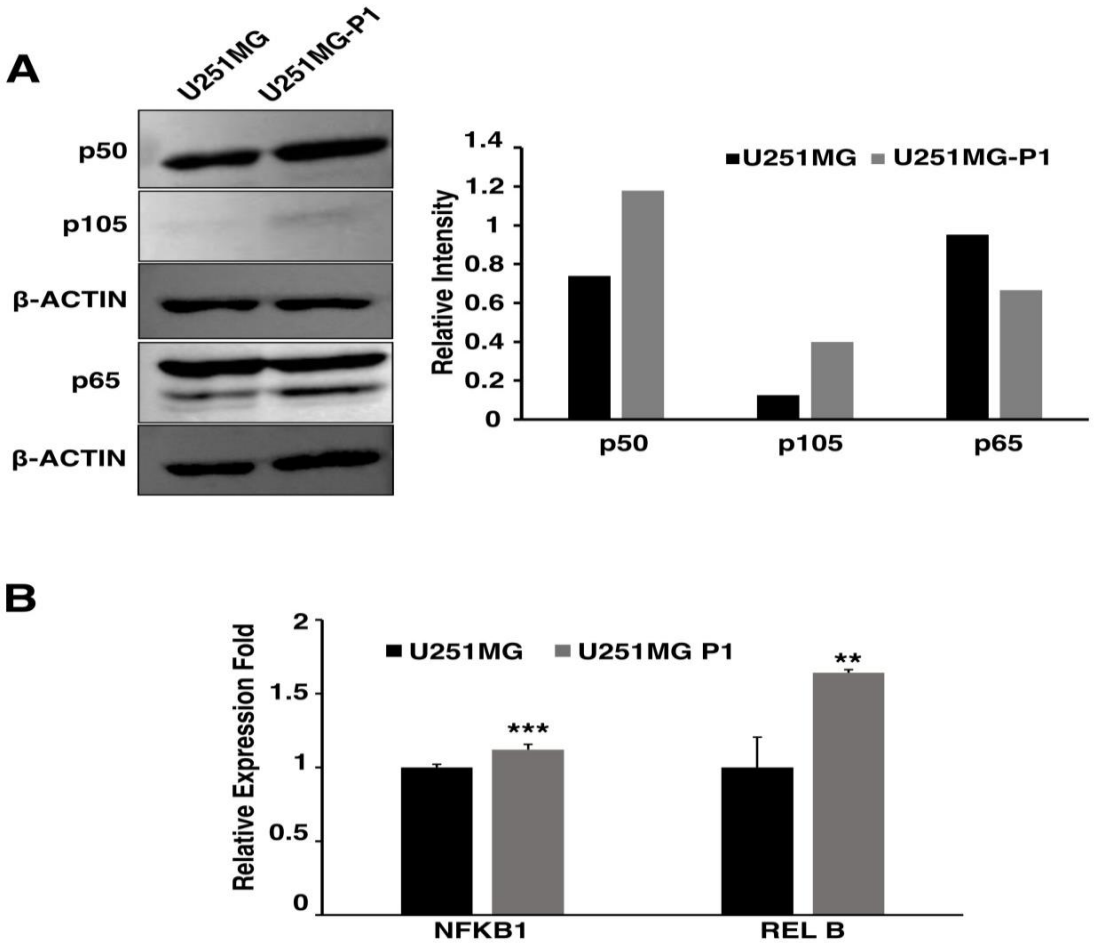

Figure 8: Activation of inflammation and angiogenic mediators. (A) U251MG and U251MG-P1 were subjected to SDS-PAGE and were immunoblotted for p50/105 and p65. Beta actin was included as loading control for the experiment. Normalized band intensity were plotted as a bar graph using Image J (B) qPCR was performed with the designated primers in Table 1 (Material and method).

3.5 Analysed of tumor tissue (U251MG-P1).

3.5.1 Differentation marker (GFAP) and immunohistochemical analysis

To evaluate the extent of differentiation in these tumors, the glial fibrillary acidic protein (GFAP), a marker used to distinguish astrocytes from glial cells which also is a progenitor marker for the neural stem cells (NSCs) were analysed. In our hands, the GFAP expression is reduced in the U251MG-P1 cells which might be due to the enrichment of the undifferentiated stem-like the population in the primary tumor from the mouse To further probe the stability of the GFAP expression in the tumor, we subsequently retransplanted the tumor to the mice and were further confirmed with the Western blot (**Figure 9A**).

Immunohistochemical analysis showed the exend of angiogenesis induction along with the presence of CD133+ cells intercalated throughout the tumor. We further probed for the expression of LYVE-1 expression to check the lymphangiogenesis in the tumor and in our hands, the LYVE-1 expression was very much limited in the tumor .

Hispathological and gene expression analysis have further confirmed the similar characteristic of the parental cancer cell lines (**Figure 9B**).

Similar studies have been conducted in breast and colon cancer previously [19, 28] along with combining the genetic model with xenograft transplantations [29]. Similar studies has shown that the CD133+ conditioned media in glioma enhances the angiogenesis in patient xenografts in mouse by elevated VEGF expression and endothelial differentiation thereby the presence of stem cell populations determines the key events in angiogenesis and vascular mimicry [30-32]. Similar model system was generated using miPS cells by our group where the angiogenesis/vascular mimicry were a cooperative interaction between the CSC and the microenvironment comprising of the differentiated populations, including the endothelial cells, and tumor stroma [33].

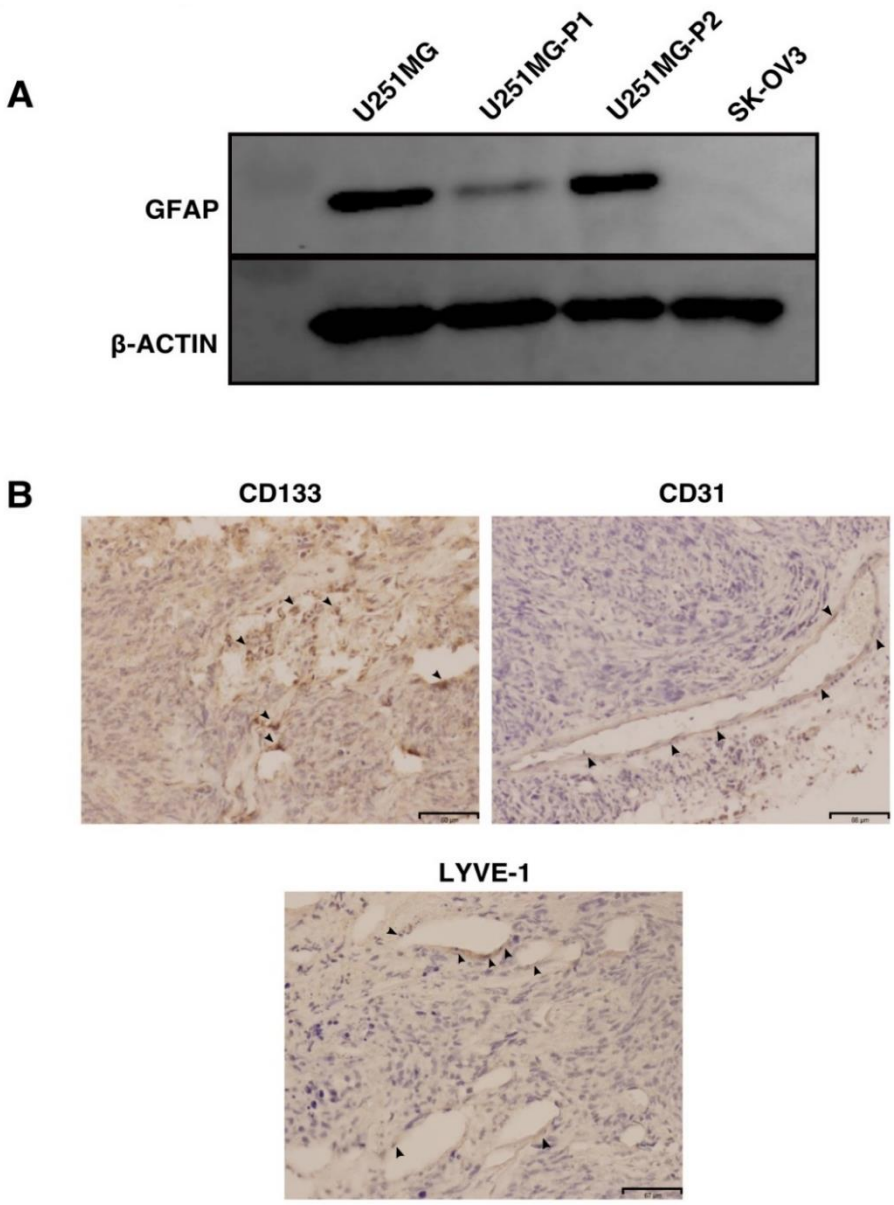

Figure 9 : Characterization of the tumor in the mouse. (A) To check the extent of the differentiation in the tumor we compared the GFAP by western blotting in the parental, primary and secondary tumor culture *in vitro*. SK-OV-3 cell lysate was included as a negative control for the experiment. (B) Representative data for the immunohistochemical

analysis of the frozen tumor sections with anti-CD133, anti-CD31 and anti-LYVE-1 antibodies. Scale Bar: 80 μm.

4.0 Conclusion

Xenograft models give more simultaneity and reproducibility with their high incidence of the tumor formation. Also they allow easy tumor visualization for the drug development process and efficient penetrance of the drug interactions with the tumor [34, 35]. Enrichment of CD44 expressing cells would be a better platform in the drug targeting experiments for CSCs as we previously successfully showed targeting HER2 breast cancer cells with our bionanocapsule [36] and liposome [37, 38] with HER2-binding artificial ligands and such models will provide extensive knowledge in the therapeutic intervention in curbing the cancer growth and metastasis. The advantage of our model involves its cost-effective enrichment of the CD44 expressing glioblastoma cells and high tumor incidence within a short time, enables us to study the effect of chemotherapeutic targeting. Further, the development of the mouse model will assist in the molecular targeting using anti-CD44 antibody-drug encapsulated nanoparticles for glioma CSCs**.**

References

1. The Cancer Genome Atlas Research, N., *Comprehensive genomic characterization defines human glioblastoma genes and core pathways.* Nature, 2008. **455**(7216): p. 1061-1068.
2. Louis, D.N., et al., *The 2007 WHO Classification of Tumours of the Central Nervous System.* Acta Neuropathologica, 2007. **114**(2): p. 97-109.
3. (2011, M.W.a.M.V.R., *Matrix Microenvironment in Glioma Progression, Glioma* in *Glioma - Exploring Its Biology and Practical Relevance*. 2011, InTech.
4. Changyou, Z. and L. Weiyue, *The Blood-Brain/Tumor Barriers: Challenges and Chances for Malignant Gliomas Targeted Drug Delivery.* Current Pharmaceutical Biotechnology, 2012. **13**(12): p. 2380-2387.
5. Plaks, V., N. Kong, and Z. Werb, *The Cancer Stem Cell Niche: How Essential Is the Niche in Regulating Stemness of Tumor Cells?* Cell Stem Cell. **16**(3): p. 225-238.
6. Nguyen, L.V., et al., *Cancer stem cells: an evolving concept.* Nature Reviews Cancer, 2012. **12**: p. 133.
7. Egeblad, M., E.S. Nakasone, and Z. Werb, *Tumors as Organs: Complex Tissues that Interface with the Entire Organism.* Developmental Cell, 2010. **18**(6): p. 884-901.

8. Tammi, R.H., et al., *Hyaluronan in human tumors: Pathobiological and prognostic messages from cell-associated and stromal hyaluronan.* Seminars in Cancer Biology, 2008. **18**(4): p. 288-295.

9. Auvinen, P., et al., *Hyaluronan synthases (HAS1–3) in stromal and malignant cells correlate with breast cancer grade and predict patient survival.* Breast Cancer Research and Treatment, 2014. **143**(2): p. 277-286.

10. Sugli, Y., et al., *A Unique Procedure to Identify Cell Surface Markers through a Spherical Self-Organizing Map Applied to DNA Microarray Analysis.* Biomarkers in Cancer, 2016. **8**: p. BIC.S33542.

11. Chanmee, T., et al., *Excessive Hyaluronan Production Promotes Acquisition of Cancer Stem Cell Signatures through the Coordinated Regulation of Twist and the Transforming Growth Factor β (TGF-β)-Snail Signaling Axis.* Journal of Biological Chemistry, 2014. **289**(38): p. 26038-26056.

12. Schatton, T., N.Y. Frank, and M.H. Frank, *Identification and targeting of cancer stem cells.* BioEssays, 2009. **31**(10): p. 1038-1049.

13. Ponta, H., L. Sherman, and P.A. Herrlich, *CD44: From adhesion molecules to signalling regulators.* Nature Reviews Molecular Cell Biology, 2003. **4**: p. 33.

14. Pietras, A., et al., *Osteopontin-CD44 Signaling in the Glioma Perivascular Niche Enhances Cancer Stem Cell Phenotypes and Promotes Aggressive Tumor Growth.* Cell Stem Cell, 2014. **14**(3): p. 357-369.

15. Yang, C., et al., *The High and Low Molecular Weight Forms of Hyaluronan Have Distinct Effects on CD44 Clustering.* Journal of Biological Chemistry, 2012. **287**(51): p. 43094-43107.

16. Zöller, M., *CD44: can a cancer-initiating cell profit from an abundantly expressed molecule?* Nature Reviews Cancer, 2011. **11**: p. 254.

17. Gao, F., et al., *Hyaluronan oligosaccharides are potential stimulators to angiogenesis via RHAMM mediated signal pathway in wound healing*. Vol. 31. 2008. E106-16.

18. Wang, Y.Z., et al., *CD44 mediates oligosaccharides of hyaluronan-induced proliferation, tube formation and signal transduction in endothelial cells.* Experimental Biology and Medicine, 2011. **236**(1): p. 84-90.

19. Singh, S.K., et al., *Cancer stem cells in nervous system tumors.* Oncogene, 2004. **23**: p. 7267.

20. Olmez, I., et al., *Dedifferentiation of patient-derived glioblastoma multiforme cell lines results in a cancer stem cell-like state with mitogen-independent growth.* Journal of Cellular and Molecular Medicine, 2015. **19**(6): p. 1262-1272.

21. Bourguignon, L.Y.W., et al., *Hyaluronan-CD44 Interaction with Protein Kinase Cϵ Promotes Oncogenic Signaling by the Stem Cell Marker Nanog and the Production of MicroRNA-21, Leading to Down-regulation of the Tumor Suppressor Protein PDCD4, Anti-apoptosis, and Chemotherapy Resistance in*

Breast Tumor Cells. Journal of Biological Chemistry, 2009. **284**(39): p. 26533-26546.

22. Bourguignon, L.Y.W., et al., *Hyaluronan-CD44 Interaction Activates Stem Cell Marker Nanog, Stat-3-mediated MDR1 Gene Expression, and Ankyrin-regulated Multidrug Efflux in Breast and Ovarian Tumor Cells.* Journal of Biological Chemistry, 2008. **283**(25): p. 17635-17651.
23. Chambers, I., et al., *Functional Expression Cloning of Nanog, a Pluripotency Sustaining Factor in Embryonic Stem Cells.* Cell, 2003. **113**(5): p. 643-655.
24. Bhat, Krishna P.L., et al., *Mesenchymal Differentiation Mediated by NF-κB Promotes Radiation Resistance in Glioblastoma.* Cancer Cell. **24**(3): p. 331-346.
25. Lee, D.W., et al., *The NF-κB RelB Protein Is an Oncogenic Driver of Mesenchymal Glioma.* PLOS ONE, 2013. **8**(2): p. e57489.
26. Sen, E., *Targeting inflammation-induced transcription factor activation: an open frontier for glioma therapy.* Drug Discovery Today, 2011. **16**(23): p. 1044-1051.
27. Nogueira, L., et al., *Blockade of the NFκB pathway drives differentiating glioblastoma-initiating cells into senescence both in vitro and in vivo.* Oncogene, 2011. **30**: p. 3537.
28. Singh, S.K., et al., *Identification of a Cancer Stem Cell in Human Brain Tumors.* Cancer Research, 2003. **63**(18): p. 5821-5828.

29. Harris, M.A., et al., *Cancer Stem Cells Are Enriched in the Side Population Cells in a Mouse Model of Glioma.* Cancer Research, 2008. **68**(24): p. 10051-10059.

30. Bao, S., et al., *Stem Cell–like Glioma Cells Promote Tumor Angiogenesis through Vascular Endothelial Growth Factor.* Cancer Research, 2006. **66**(16): p. 7843-7848.

31. Ming-Tsang, C., et al., *CD133+ Glioblastoma Stem-Like Cells Induce Vascular Mimicry in Vivo.* Current Neurovascular Research, 2011. **8**(3): p. 210-219.

32. Ricci-Vitiani, L., et al., *Tumour vascularization via endothelial differentiation of glioblastoma stem-like cells.* Nature, 2010. **468**: p. 824.

33. Prieto-Vila, M., et al., *iPSC-derived cancer stem cells provide a model of tumor vasculature.* American Journal of Cancer Research, 2016. **6**(9): p. 1906-1921.

34. Fomchenko, E.I. and E.C. Holland, *Mouse Models of Brain Tumors and Their Applications in Preclinical Trials.* Clinical Cancer Research, 2006. **12**(18): p. 5288-5297.

35. Chen, J., Renée M. McKay, and Luis F. Parada, *Malignant Glioma: Lessons from Genomics, Mouse Models, and Stem Cells.* Cell, 2012. **149**(1): p. 36-47.

36. Vaidyanath, A., et al., *Enhanced internalization of ErbB2 in SK-BR-3 cells with multivalent forms of an artificial ligand.* Journal of Cellular and Molecular Medicine, 2011. **15**(11): p. 2525-2538.

37. Shigehiro, T., et al., *Efficient Drug Delivery of Paclitaxel Glycoside: A Novel Solubility Gradient Encapsulation into Liposomes Coupled with Immunoliposomes Preparation.* PLoS ONE, 2014. **9**(9): p. e107976.

38. Shigehiro, T., et al., *Evaluation of glycosylated docetaxel-encapsulated liposomes prepared by remote loading under solubility gradient.* Journal of Microencapsulation, 2016. **33**(2): p. 172-182.

Chapter 3

Targeting Glioblastoma Cells Expressing CD44 with Liposomes Encapsulating Doxorubicin and Displaying Chlorotoxin-IgG Fc Fusion Protein

LIST OF ABBREVIATIONS AND ACRONYMS

BBB	Blood Brain Barrier
CTX	Chlorotoxin
CM	Conditioned media
GBM	Glioblastoma Multiforme
DAPI	4',6-diamidino-2-phenylindole
DDS	Drug delivery systems
DMEM	Dulbecco`s Modified Eagle`s medium
Dox	Doxorubicin
FBS	Fetal bovine serum
E.coli	*Escherichia coli*
HEPES	(4-(2-hydroxyethyl)-1-piperazineethanesulfonic acid)
h	hours
hIgG-L-Dox	Liposome conjugated with human IgG encapsulating doxorubicin
IC_{50}	Half Maximal Inhibitory Concentration
IgG	Immunoglobulin G
IU	International Unit
L-Dox	Liposome encapsulating doxorubicin without ligand
nM	nanoMolar

nm	nanometer
M-CTX-Fc	Chlorotoxin peptide fused to human IgG Fc region
M-CTX-Fc-L-Dox	Liposome conjugated with M-CTX-Fc encapsulating doxorubicin
MMP-2	Matrix metalloprotease-2
MLV	Multilamellar Vesicles
min	minutes
MTT	3-(4,5-dimethylthiazol-2-yl)-2,5-diphenyltetrazolium bromide
PBS	Phosphate Buffered Saline
RES	Reticuloendothelial system
RPMI	Roswell Park Memorial Institute medium

LIST OF TABLE

LIST OF FIGURES

Abstract

We recently have established a successful xenograft model of human glioblastoma cells by enriching hyaluronic acid-dependent spheroid-forming populations termed U251MG-P1 cells from U251MG cells. Since U251MG-P1 cells have been confirmed to express CD44 along with principal stemness marker genes, *OCT3/4*, *SOX2*, *KLF4* and *Nanog*, this CD44 expressing population appeared to majorly consist of undifferentiated cells. Evaluating the sensitivity to anti-cancer agents, we found U251MG-P1 cells were sensitive to doxorubicin with IC50 at 200 nM. Although doxorubicin has serious side-effects, establishment of an efficient therapy targeting undifferentiated glioblastoma cell population is necessary. We previously designed a chlorotoxin peptide fused to human IgG Fc region without hinge sequence (M-CTX-Fc), which exhibited a stronger growth inhibitory effect on the glioblastoma cell line A172 than an original chlorotoxin peptide. Combining these results together, we designed M-CTX-Fc conjugated liposomes encapsulating doxorubicin and used U251MG-P1 cells as the target model in this study. The liposome modified with M-CTX-Fc was designed with a diameter of approximately 100–150 nm and showed high encapsulation efficiency, adequate loading capacity of anticancer drug, enhanced antitumor effects, demonstrating increasing uptake into the cells in vitro; M-CTX-Fc-L-Dox shows great promise in its ability to suppress tumor growth in vivo and it could serve as a template for targeted delivery of other therapeutics.

Graphical Abstract

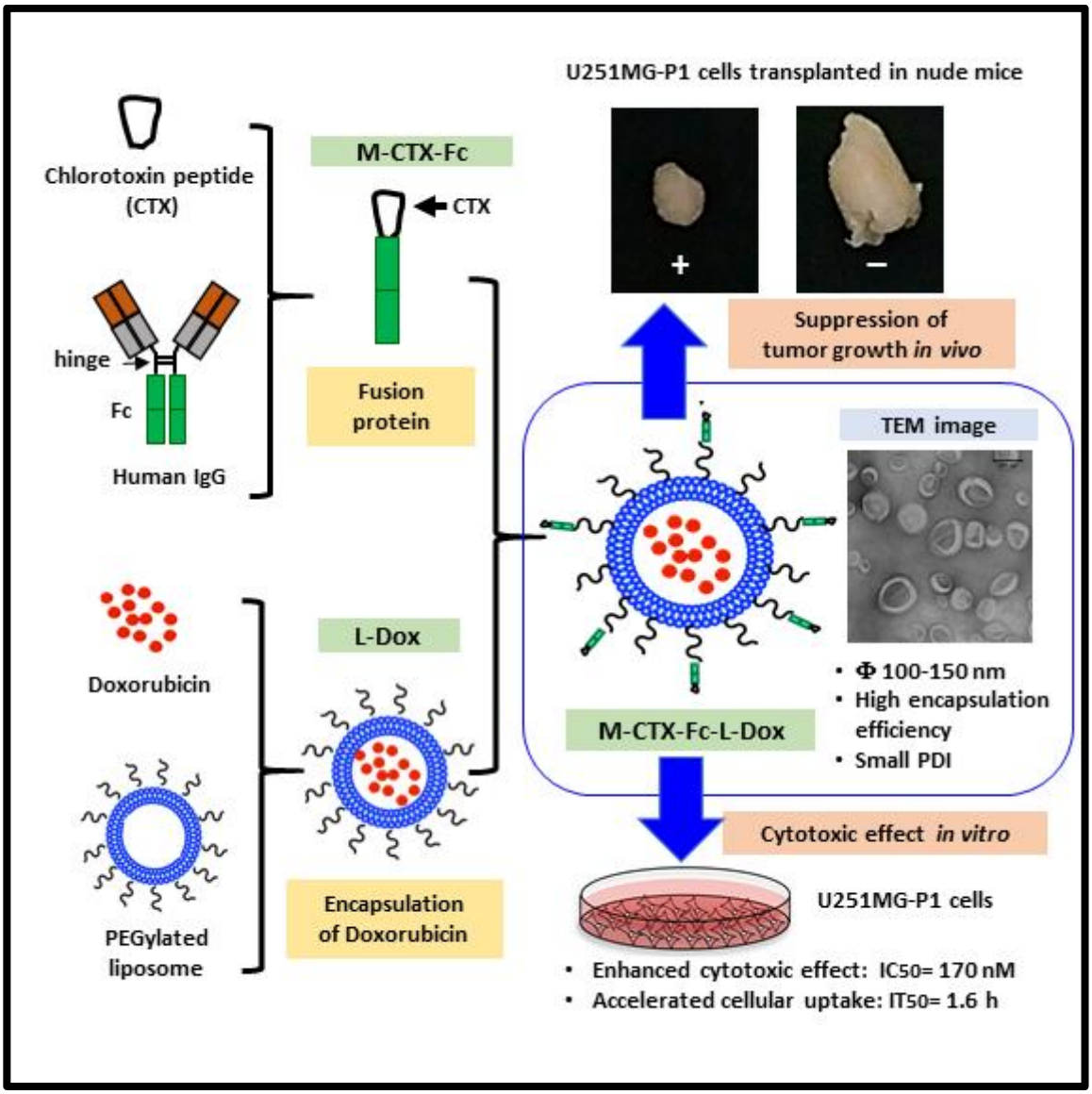

1.0 Introduction

Glioblastoma is a highly invasive cancer where the cells demonstrate their infiltrative growth to diffuse into the brain tissue [1]. This is the reason why the treatment of glioblastoma requires a multidisciplinary approach. Current standard of care for glioblastoma includes maximal safe surgical resection followed by radiotherapy and chemotherapy with alkylating agents, Temozolomide. The extensive and complete surgical treatment involves difficulties in glioblastoma with high degree of invasion because simultaneous removal of the surrounding normal areas will impair the function of brain controlling speech, motor function, sense and personality [2]. On that occasion, developing of brain tumor specific targeting drug delivery systems, which increase drug accumulation in the tumor region with less toxicity to the adjacent normal brain tissue, would significantly be a great approach for brain tumor treatments. The drug delivery to brain faces has been considered difficult as the agents need to across the blood brain barrier (BBB). However, recent study has shown that the tight junction of BBB loses the integrity by increasing permeability of the capillary endothelium [3].

On the other hand, recurrence of relapsing cancer is currently the central big issue to be studied. This is considered to occur due to the residual subpopulation of cancer cells after the treatment because they are believed to be resistant to the chemotherapy and radiotherapy even they are the minor population in the cancer tissues [4] . In this context,

chemical agents toxically effective to cancer cells should properly be chosen to design the effective drug delivery system.

As for the efficacy of the drug delivery, targeting ability is another strong issue to be designed. Some cell surface antigens including receptors specific to gliomas and/or neovasculatures will be crucial markers to be targeted [5]. Hence, several approaches to treat brain cancer employ ligands specific to the tumor cells targeting the cell surface markers, which are overexpressed in cancer cells but low or not expressed in normal cells.

Matrix metalloprotease-2 (MMP-2) is an extracellular matrix degrading enzyme, which play an important role in tumor invasion and is highly expressed in related cancer cells [6]. As for the MMP-2 in glioblastoma, the activity is increased along with the tumor grade and the expression is significantly higher than that in normal brain tissue. The increment is associated with the poor prognosis and overall short-life of survivors. MMP-2 are secreted as an inactive zymogen and prior to its activation, it will bind to tissue inhibitor of metalloproteinase-2 associated with membrane type matrix metalloproteinase-1, which localizes on the cell surface of the tumors [7, 8]. Membrane type matrix metalloproteinase-1 is replenished by auto degradation or clathrin-dependent internalization. Collectively, MMP-2 has been considered as a target for cancer therapy.

Chlorotoxin (CTX) is a peptide derived from Egyptian scorpion venom, which has initially been characterized as a MMP-2 inhibitor and also as a voltage-gated chloride channel blocker [9, 10]. CTX exhibited high specificity, selectivity and affinity for glioma and other tumor of neuroectodermal origin [11]. Following the discovery, CTX has been

extensively developed as a ligand for active targeting to deliver cytotoxic agent, fluorescent dye for imaging and iodine for labeling to tumor cells [12-14]. Recent finding suggested that the delivery of CTX-modified liposome was mediated by MMP-2 but not correlated with the chloride channel CIC-3 when targeting U87 glioma cells [15].

In our previous report, the CTX fused to human IgG Fc domain without hinge region in monomeric form (M-CTX-Fc) showed inhibition of mortality of glioma cell line A172 cells [16]. This inhibitory effect was enhanced when compared to the original CTX peptide. The similar effect was observed in pancreatic cancer cell PANC-1 cells [17]. Indicating M-CTX-Fc could be a potential ligand for active targeting of glioblastoma cells, the target-dependent internalization of bionanocapsules displaying M-CTX-Fc on the surface into cells was described [16].

Very recently, we condensed the population overexpressing CD44 in U251MG cells exploiting the preferential affinity for hyaluronic acid as U251MG-P1 cells [18]. Since CD44 is well known as a common marker of cancer stem cells, we confirmed the expression of stemness markers as well as the tumor-initiating capacity in U251MG-P1 cells

In this study, we designed the liposomal drug delivery system of doxorubicin to evaluate the ability of M-CTX-Fc as an effective moiety to target glioblastoma cells expressing stemness markers using U251MG-P1 cells as the target model.

2.0 Materials and Methods

2.1 Materials

Dipalmitoylphosphatidylcholine (DPPC),1,2-distearoyl-sn-glycerol-3 phosphoethanolamine-N-[methoxy (polyethylene glycol)-2000] (mPEG–DSPE) and 1,2-distearoyl-sn-glycerol-3-phosphoethanolamine-N-[maleimide (polyethylene glycol)-2000] (Mal–PEG–DSPE) were obtained from NOF Co. (Tokyo, Japan). Cholesterol (Chol) was purchased from Kanto Chemical Co., Inc. (Tokyo, Japan). Thiazolyl blue tetrazolium bromide (MTT), 2-iminothiolane hydrochloride, human IgG, RPMI 1640 medium, and DMEM were from Sigma-Aldrich (St Louis, MO, USA). Doxorubicin hydrochloride was purchased from Wako Pure Chemical (Osaka, Japan). Amicon Ultra filters were from Merck Millipore Ltd. (Billerica, MA, USA). PD-10 columns were from GE Healthcare (Carlsbad, CA, USA).

2.2 Cell Cultures and Experimental Animals

The human glioblastoma cell line A172 cells and human breast cancer cell line SK-BR-3 cells were obtained from ATCC (Manassas, VA, USA). U251MG-P1 was isolated from a xenograft tumor of human glioblastoma cell line U251MG cells in mouse [18]. A172 and U251MG-P1 were maintained in DMEM medium supplemented with 10%

fetal bovine serum (FBS) (PAA Laboratories, Pasching, Austria) in the presence of 100 IU/mL penicillin and 100 μg/mL streptomycin (Nacalai Tesque, Kyoto, Japan). SK-BR-3 cells were cultured in RPMI 1640 medium supplemented with 10% FBS in the presence of 100 IU/mL penicillin and 100 μg/mL streptomycin. Cells were cultured in a humidified incubator at 37°C with the atmosphere of 5% CO2.

Four-week-old female BALB/c nude mice from Charles River (Kanagawa, Japan) were bred at 23 ˚C and fed with sterilized food and water during the experiments. All animal experimental protocols were reviewed and approved by the ethics committee known as IACUC (Institutional Animal Care and Use Committee) of Okayama University under project identification code OKU-2016078 (Date of approval :1 April 2016).

2.3 Preparation of M-CTX-Fc

M-CTX-Fc fusion protein was produced in our laboratory by recombinant expression in *E.coli* [14,15]. Briefly, M-CTX-Fc was expressed in *E.coli* as inclusion body and was refolded *Escherichia coli* BL21 (DE3) pLysS (Novagen) was transformed with expression vectors for M-CTX-Fcs**.** Transformants were grown in 1 L of LB medium containing 50 μg/mL kanamycin and 10 μg/mL chloramphenicol at 37 °C. Protein expression was induced by 0.4mM isopropyl 1-thio-β-D-galactopyranoside. After expression induction, the transformants were cultured at 25°C for 16 h, and the bacteria were harvested. Cell pellets were thawed and homogenized in 20mL of lysis buffer

containing 10mM Tris-HCl (pH 8.0), 10mM EDTA, 0.2M NaCl, and 10% sucrose. The inclusion bodies were collected by centrifugation at 12,000 × g for 20 min.

The inclusion bodies were washed three times with 0.5% Triton X-100. The insoluble fraction was resolved in 4 mL of 6M guanidinium HCl containing 0.1M Tris-HCl (pH 8.5). The solution was degassed by aspiration while purging the air with nitrogen gas and supplemented with 50 μL of 2-mercaptoethanol. After 1 h incubation at 37°C in a shaking water bath, the mixture was dispersed into a 20-fold volume of refolding buffer containing 10mM Tris-HCl (pH 8.5), 0.1M NaCl, and 0.5mM oxidized glutathione. Refolding was conducted by incubation at 4 °C for 18 h. The pH was then adjusted to 7.0 using acetic acid. Insoluble materials were removed by centrifugation at 12,000×g for 20 min. The solution containing refolded protein was applied to a cobalt resin column (TALON superflow metal affinity resin, Clontech, Mountain View, CA, USA), after equilibrating with equilibration buffer containing 50mM phosphate buffer (pH 7.0) and 300mM NaCl. The column was then washed with equilibration buffer containing 20mM imidazole and 0.1% Triton X-100. M-CTX-Fcs were eluted with elution buffer containing 50mM phosphate buffer (pH 7.0), 300mM imidazole, and 300mM NaCl. The eluted solution was dialyzed three times against phosphate-buffered saline (Dulbecco's formula, hereafter PBS) for 2 h each time. The purity of M-CTX-Fcs in the final preparations was assessed by SDS-PAGE, Coomassie Brilliant Blue (CBB) staining, and western blotting **(Figure S1 in Supplementary Material)**.

2.4 Gelatin zymography for MMP-2 activity

MMP-2 gelatinolytic activity in the CM was determined by zymography. Fifteen microliter aliquots of CM with or without M-CTX-Fc were subjected to 10 % SDS-PAGE containing 0.05% gelatine. The samples were prepared without reducing reagent and boiling prior to electrophoresis. After electrophoresis, the gel was washed twice in 2.5 % Triton X-100 for 30 min and once in 50 mM Tris-HCI, pH 7.4, 10 mM CaCl2 and 0.02 % NaN3. After incubation, gel was stained with Coomassie brilliant blue in 50 % methanol and 10 % acetic acid and destained in 10% methanol and 10% acetic acid.

2.5 Preparation of liposomes encapsulating doxorubicin

2.5.1 Encapsulation of doxorubicin into liposomes

Liposomes composed of DPPC and chol with 5 mol% mPEG-DSPE were prepared by the thin-film hydration method followed by the transmembrane pH gradient method [19, 20]. In brief, DPPC, Chol, and mPEG-DSPE were dissolved in an organic solvent mixture consisting of chloroform and methanol (9:1, v/v) in a round-bottom flask equipped with rotary evaporator at 50˚C under aspirator vacuum. The resulting lipid film was left overnight under vacuum to ensure that all traces of organic solvent are removed from the film. Then, the film was hydrated with 300 mM citrate buffer, pH 4.0, by gentle mixing, resulting in spontaneously organized multilamellar vesicles (MLVs). MLVs were

freeze-thawed five times and passed through a Whatman polycarbonate membrane with a pore size of 100 nm (GE Healthcare, Carlsbad, CA) ten times using an extruder (Avanti Polar Lipids, Inc., Alabaster, AL) to form small, unilamellar vesicles. The liposome suspension was eluted using Sephadex G-25 (PD-10 desalting column) pre-equilibrated with PBS, pH 7.4, to form a pH gradient. Dox at pH 7.4 was introduced into the liposome suspension, and an excess of free Dox was removed by washing with PBS followed by ultrafiltration using a 100K-membrane filter.

2.5.2 Preparation of M-CTX-Fc-L-Dox or hIgG-L-Dox

The M-CTX-Fc or human IgG were coupling to liposome using classical method by employing the maleimide -thiol addition reaction [21]. Briefly, 2 mol% of Mal-PEG-DSPE were incubated with Dox loaded liposome at 50 ˚C for 10 min. Simultaneously, thiol group (-SH) were introduced into M-CTX-Fc and human IgG by incubation with Traut's reagent (2-iminothiolane) at molar ratio of 1:10 and 1:50 in 25 mM HEPES, pH 8.0, containing 140 mM NaCI respectively. The reaction occurred under gentle stirring for 1 h in the dark at room temperature. Unreacted 2-IT reagent was removed by using gel chromatography G25 PD-10 column (GE Healthcare, Carlsbad, CA). Thiolated M-CTX-Fc or human IgG was then coupled to Mal-PEG-DSPE by thioether linkage. The coupling reaction was performed overnight in the dark with gentle stirring at 4 ˚C. Free M-CTX-Fc

or human hIgG was removed by ultrafiltration with 100K and 300K membrane filter respectively (Sartorius Stedim Biotech GmbH, Gotttingen) (**Figure S2**).

2.6 Characterization of liposomes

2.6.1 Size distribution and zeta potential

The size and zeta potential of liposomes were determined by dynamic and electrophoretic light scattering using an ELS-8000 (Photal Otsuka Electronic, Osaka, Japan).

2.6.2 Encapsulation efficiency (EE) and loading efficiency (LE)

The concentration of Dox was quantified by UV-VIS spectrophotometry (Corona Electric, Ibaraki, Japan) at 490 nm. EE was then calculated as the amount of drug loaded in the liposomes divided by initial amount of the drug. LE was calculated as the molar ratio of the drug loaded into liposomes to the total of lipid and Chol.

2.7 Evaluation of cellular uptake of liposomes

The cellular uptake of liposomes was evaluated according to the previously described method [15]. U251MG-P1 and SK-BR-3 cells were cultured on gelatin-coated

glass coverslips in a 12-well plate at a density of 3 x 10^5 cells per well for 24 h. Then, M-CTX-Fc and L-Dox (containing Dox at 30 μg/mL) were added to a serum-free medium and incubated at 37 °C in the darkness for 1 h. The cells treated with a medium were used as a negative control. After the incubation, cells were washed three times with cold PBS and fixed with 4% paraformaldehyde for 20 min. After nuclear staining with DAPI (Vector Laboratories, Burlingame, CA), the fluorescent signal was imaged using a laser scanning confocal microscope (FV-1000, Olympus, Tokyo, Japan).

2.8 Cytotoxic assay

To investigate the *in vitro* cytotoxicity of various Dox-loaded liposomes in U251MG-P1 and SK-BR-3 cells, tetrazolium reduction assay was employed as previously described [22]. Briefly, 5,000 cells/well were seeded onto a 96-well plate and cultured for 24 h. Then, the cells were incubated with 50 μL of a culture medium containing free Dox or different liposome formulations with various Dox concentrations for 72 h at 37 °C and 5% CO2. Afterward, the cells were exposed to 5 mg/mL of MTT in PBS (the final concentration of 1 mg/mL) for 4 h. Formazan crystals formed during the incubation period were dissolved overnight at 37 °C by adding 10% SDS containing 20 mM HCI. The absorbance was measured at 570 nm using 96-well plate reader (Corona MTP-800, Tokyo, Japan). The exposure time required to kill 50% of the cells was evaluated as IT_{50}, which

should be obtained at the minimum concentration of doxorubicin killing 100% of the cells after 72 h of exposure defined as IC_{100}.

2.9 Time- dependent cytotoxic effects

Time-dependent cellular cytotoxicity [22] was evaluated by the MTT assay with drugs at IC_{100} (Table 1). Briefly, U251MG-P1 and SK-BR-3 were seeded in a 96-well plate at 5×10^{3} cell/well. After incubation at 37ºC under 5% CO_2 for 24 h, drugs at each IC_{100} were added to each well and incubated for 1, 2, 6, 12, 24, 48, and 72 h. After each round of drug exposure, the medium was replaced with fresh medium without drugs and the incubation was continued until 72 h. Cell viability was determined by MTT assay. The time required for 50% growth inhibition (IT_{50}) was estimated from the survival curve.

Table 1. Cytotoxicity of different Dox formulations in U251MG-P1 and SK-BR-3

	U251MG-P1			SK-BR-3		
	IC_{50} (μM)	IC_{100} (μM)	IT_{50} (h)	IC_{50} (μM)	IC_{100} (μM)	IT_{50} (h)
Dox	0.19 ± 0.11	1	2.3 ± 0.2	0.15 ± 0.02	1	3.0 ± 1.0
L-Dox	0.35 ± 0.08	5	3.4 ± 0.4	0.21 ± 0.05	1	6.0 ± 0.8
hIgG-L-Dox	0.66 ± 0.05	10	4.1 ± 0.6	0.38 ± 0.06	1	9.5 ± 0.6
M-CTX-Fc-L-Dox	0.17 ± 0.07	1	1.6 ± 0.4	0.21 ± 0.04	1	6.6 ± 1.6

IC50 and IT50 are presented as the mean ± S.D. (n = 3).
IC100 was estimated from the evaluation of cytotoxicity.

2.10 Anti-tumor study *in vivo*

The xenograft of U251MG-P1 cells in mice was prepared by a subcutaneous injection of 1 x 10^6 cells/mouse. Tumor volume was measured by a vernier caliper and calculated as [length x $(width)^2$]/2. Anti-tumor effect of each formulation was evaluated when the tumor volume reached 100-200 mm^3. Mice were randomly assigned to five groups (n = 3); group 1 for saline, group 2 for naked Dox, group 3 for L-Dox, group 4 for hIgG-L-Dox and group 5 for M-CTX-Fc-L-Dox. Ten mg of doxorubicin per kg body weight was injected three times via tail vein at the intervals of 7-day. Tumor volume was measured every three days.

2.11 Statistical analysis

All the experiments were at least three-time repetition. Data were depicted as means ± standard deviation. The statistical significance in mean values between two groups was determined by 2-tailed student`s t-test. The statistical significance between the mean values of more than two groups was determined using one-way analysis of variance (ANOVA) and post hoc Tukey HSD. A p-value less than 0.05 was considered to be statistically significant, and a p-value less than 0.01 was regarded as highly significant.

3.0 Results and Discussion

3.1 Sensitivity of U251MG-P1 Cells to Doxorubicin

First of all, we assessed the effect of doxorubicin on U251MG-P1 cells (**Figure 1**). We chose doxorubicin as the first priority because the liposomal formulation is well established by pH gradient and ammonium sulfate gradient method and has clinically been tested in the glioblastoma cancer therapy [23, 24]. As the result, MTT assay showed the IC_{50} at around 200 nM, which was a feasible concentration available as an agent for cancer chemotherapy.

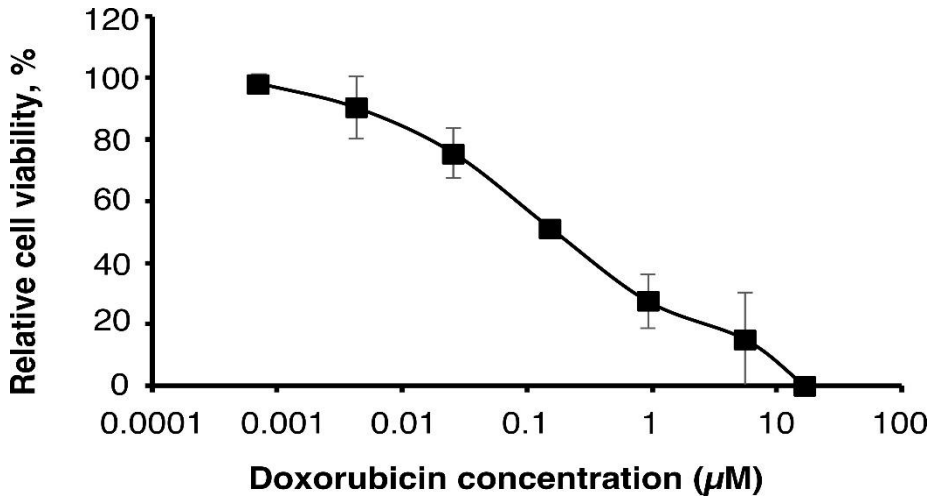

Figure 1. The U251MG-P1 cells are sensitive to doxorubicin**.** Cytotoxicity of doxorubicin was assessed on U251MG-P1 cells by MTT assay. The data presented as the mean ± S.D (n=3**)** from independent experiment.

However, cardiotoxicity is the well-known side effect of doxorubicin, so that the amount of administration through the lifetime is critically limited. If doxorubicin is one of the rare candidates of effective agents to treat such as cancer stem cells, the development of drug delivery system to avoid the side effects should seriously be important**.**

3.2. Expression of MMP-2 in U251MG-P1 cells

We assessed the expression of MMP-2 in U251MG-P1 cells to confirm that MMP-2 could be a sufficient marker to target the cells. A172 (MMP-2 positive) and human breast cancer SK-BR-3 (MMP-2 negative) cell line by both Western blot and reverse transcription-polymerase chain reaction (qRT-PCR) as shown in **Figure 2A, 1B, and 1C**. The 72 kDa protein treated with anti-MMP2 antibody corresponding to proMMP-2 was observed in U251MG-P1 and A172 but less or not seen in SK-BR-3. Since U251MG-P1 cells were confirmed to express the MMP-2, we decided to employ CTX for the specific ligand to target U251MG-P1 cells.

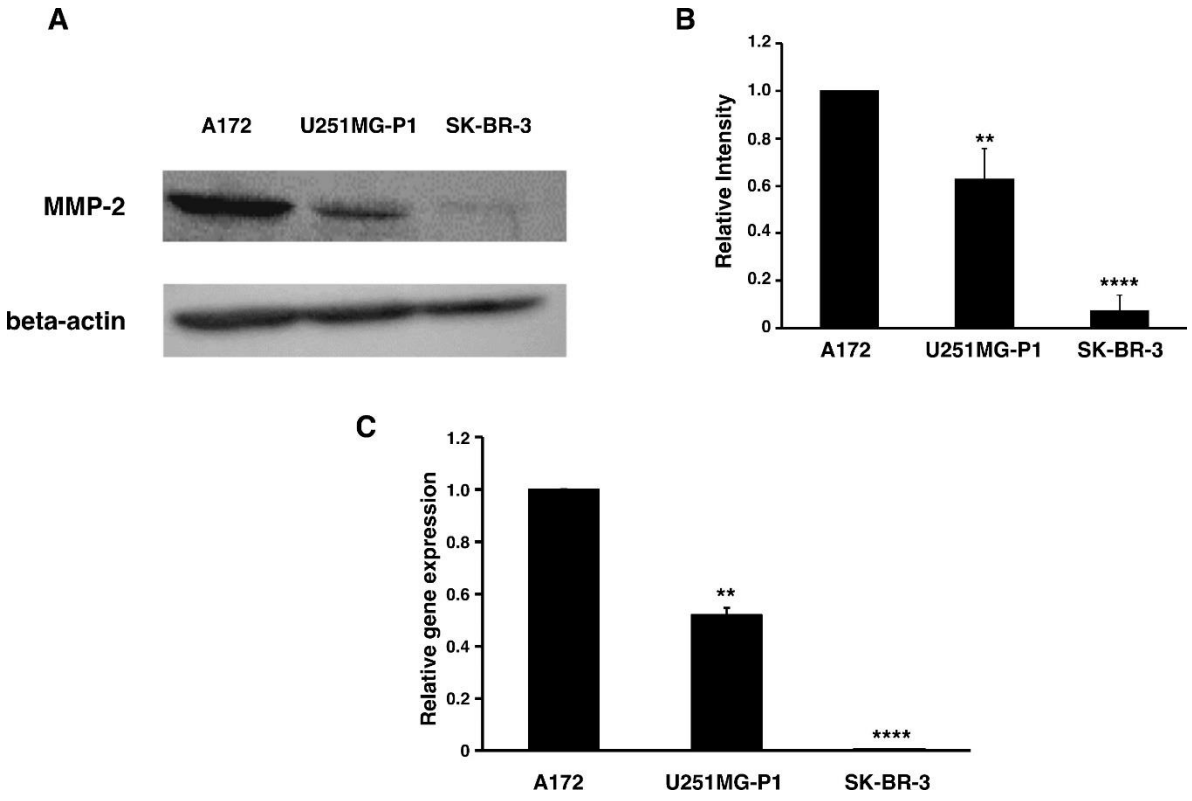

Figure 2: The U251MG-P1 cells are expressing MMP-2. A) Western blot of cells with anti-MMP-2 and anti-beta-actin antibodies, B) Relative intensity of the bands in Western blot densitometrically analyzed by ImageJ. C) Relative gene expression analyzed by reverse transcription quantitative PCR. The data presented as the mean ± S.D (n=3) from three independent experiments. The data were analyzed by 2-tailed students t-test using A172 cells as a control; *, $P<0.05$; **, $P<0.01$; ***, $P<0.005$; ****, $P<0.001$. NSD, no significant difference

3.3. Characterization of M-CTX-Fc

Peptide ligands specific to cell surface molecules have extensively been used for various drug delivery targeting cancer cells. However, they are often labile and degraded resulting in short half-life due to their antigenicity and reticuloendothelial system (RES) [25]. One of the approaches to overcome those problems is to fuse the ligand with human IgG Fc domain. The Fc domain provides significant advantages such as to improve the solubility and stability of partner molecule and to prolong the half-life in plasma [26, 27] .

After preparation of M-CTX-Fc from *E.coli*, the ability to inhibit the gelatinase activity of secreted MMP-2 in the condition medium of U251MG-P1 cells was observed by gelatin zymography (**Figure 3A**). The intensity of gelatinase activity decreased in the presence of M-CTX-Fc in a dose-dependent manner. This confirmed us the interaction of M-CTX-Fc with MMP-2 even though the exact molecular target of CTX still unknown [28]. We then evaluated the activity of M-CTX-Fc on the proliferation and viability of U251MG-P1 cells. M-CTX-Fc suppressed the growth of the cells as describe in another cells such as glioma cell line A172 cells and pancreatic canrcinoma cell line Panc-1 cells [16,17] (**Figure 3B and C**). This cell growth inhibition does not appear inducing cell death because the cell viability recovered after removal of the protein from the culture medium while CTX alone did not affect the cell growth of U251MG-P1. Collectively, we concluded that M-CTX-Fc is folded properly. Hence, we chose M-CTX-Fc in place of

CTX as the ligand to target U251MG-P1 cells considering the Fc moiety would help the conformation of CTX intact when conjugated on the surface of liposome.

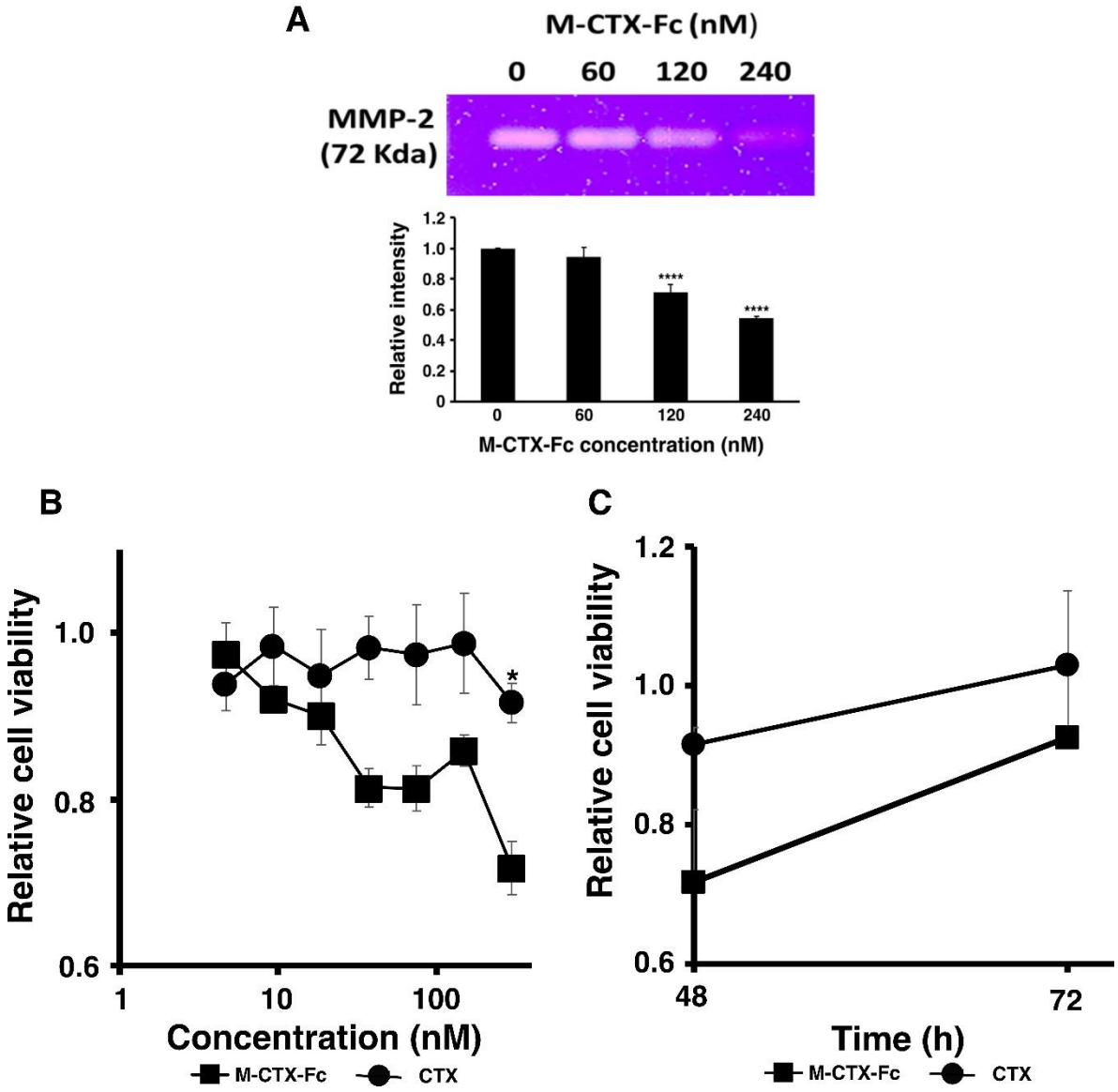

Figure 3. M-CTX-Fc inhibits gelatinase activity in the condition medium of U251MG-P1 cells (A) and cell growth of U251MG-P1 cells (B and C). The M-CTX-Fc inhibit

gelatinase activity**. A)** MMP-2 activity in the condition medium of U251MGP1 cells was monitored by zymography in the presence of 0, 60, 120, and 240 nM of M-CTX-Fc. The data presented as the mean ± S.D (n=3) from technical replicates. The statistical significance in mean values of more than two groups was determined using one-way analysis of variance (ANOVA) and post hoc Tukey HSD were applied using CM without M-CTX-Fc as control *, $P<0.05$; **, $P<0.01$; ***, $P<0.005$; ****, $P<0.001$. NSD, no significant difference. B) The inhibition of cell growth in the presence of M-CTX-Fc and CTX after 48 h. C) The viable cells at 48 h were kept cultured without M-CTX-Fcs or CTX up to 72 h. Cell numbers in each well were assessed by MTT assay. The absorbance at 570 nm corresponding to the initial number of the cells was defined as 1. The data presented as the mean ± S.D (n=3) from three independent experiments. The data were analyzed by 2-tailed students t-test using M-CTX-Fc as a control; *, $P<0.05$; **, $P<0.01$; ***, $P<0.005$; ****, $P<0.001$. NSD, no significant difference

3.4. Characterization and optimization of M-CTX-Fc conjugated to liposome.

Prior to further investigation of their cytotoxicity *in vitro* and *in vivo*, we optimized the amount of M-CTX-Fc (nmol) conjugated to liposome. The preparation of liposomes conjugated with M-CTX-Fc encapsulating doxorubicin (M-CTX-Fc-L-Dox) is summarized in Figure 4A. Various amount of M-CTX-Fc such as 5 nmol, 10 nmol, 15 nmol or 20 nmol conjugated to liposome encapsulating doxorubicin was prepared,

respectively. The mean particle size of these liposome were almost 150 nm, which was not significantly affected by the amount of ligand as previously described [29, 30]. The optimal amount of M-CTX-Fc conjugated to liposome was determined by the IC_{50} (Figure 4B). When 10 nmol of M-CTX-Fc were used to conjugate to liposome, the cytotoxicity of doxorubicin was the maximum whereas 5 nmol was not enough for binding with receptor. Similarly, M-CTX-Fc at 15 nmol and 20 nmol did not improve the cytotoxic effect of liposome encapsulating doxorubicin. We further investigated the capability of specific targeting of liposome by using M-CTX-Fc at 10 nmol.

The characteristics of the formulations of liposomes encapsulating doxorubicin used in this study were summarized in Table 2. The liposomes conjugated with human IgG (hIgG-L-Dox) or without ligands (L-Dox) were prepared as references of nonspecific targeting. All the prepared liposomes showed diameters approximately 150 nm with low polydispersity index less than 0.1 indicating homogeneous uniformity. The uniformity of particle size is considered important to obtain the stable receptor-mediated endocytosis in the intracellular delivery by the nano-carrier system [31]. The particle size between 50 and 200 nm is considered sufficient to accumulate the drug in the tumor via enhanced permeability and retention (EPR) effect since particles with larger size are generally trapped by the RES resulting in short half-life by rapid clearance from blood flow [32].

Tranmission electron microscopy (TEM) revealed that all the formulation of liposome encapsulating doxorubicin exhibited precipitates of fibrous-bundle aggregates

when doxorubicin was encapsulated into the inner core of liposome the loading method of pH gradient (Figure 5) [19].

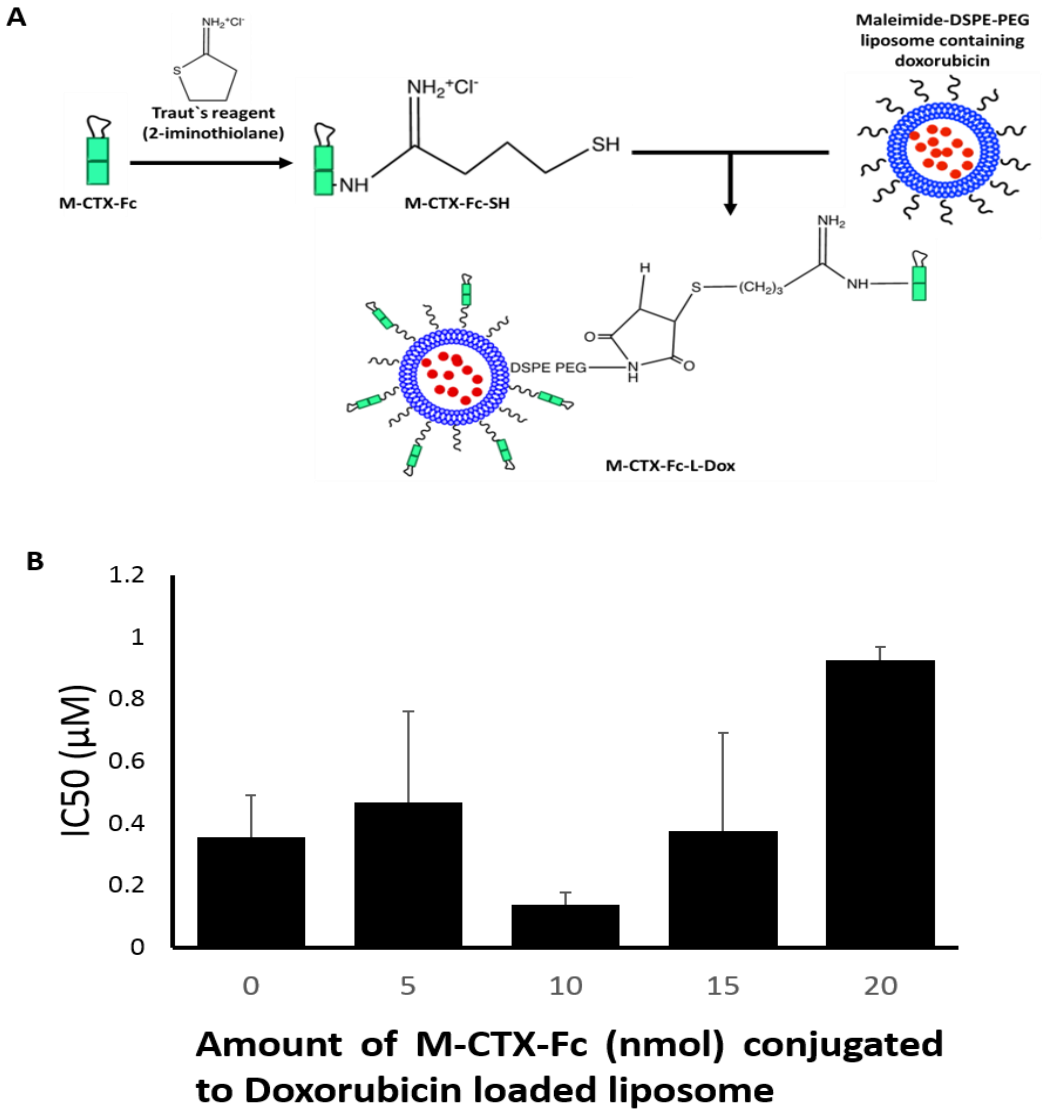

Figure 4. The amount of M-CTX-Fc conjugated to liposomes encapsulating doxorubicin was optimal at 10 nmol / 48 µmol DPPC**.** (A) Conjugation procedure of M-CTX-Fc to

liposomes encapsulating doxorubicin. (B) IC_{50} of doxorubicin encapsulated in liposomes conjugating various amount of M-CTX-Fc) against U251MG-P1 cells**.** The data presented as the mean ± S.D (n=3) from independent experiments. The statistical significance in mean values of more than two groups was determined using one-way analysis of variance (ANOVA) and post hoc Tukey HSD were applied using no M-CTX-Fc (0 mol) as control. *, P<0.05; **, P<0.01; ***, P<0.005; ****, P<0.001. NSD, no significant difference.

Table 2. Characteristics of the formulations of liposomes encapsulating doxorubicin

Formulations	**Diameter (nm)**	**Polydispersity index**	**Zeta potential (-mV)**	**Encapsulation Efficiency (%)**	**Loading Efficiency (%)**
L-Dox	133.4 ± 12.7	0.09 ± 0.03	8.13 ± 2.32	97.5 ± 3.1	3.4 ± 0.1
M-CTX-Fc-L-Dox	148.3 ± 3.0	0.05 ± 0.03	7.86 ± 1.19	98.2 ± 1.3	4.5 ± 0.4
hIgG-L-Dox	151.3 ± 4.3	0.07 ± 0.02	6.66 ± 3.78	94.4 ± 7.2	4.1 ± 0.4

Each experiment was performed in triplicate and the values are given as mean ±SD.

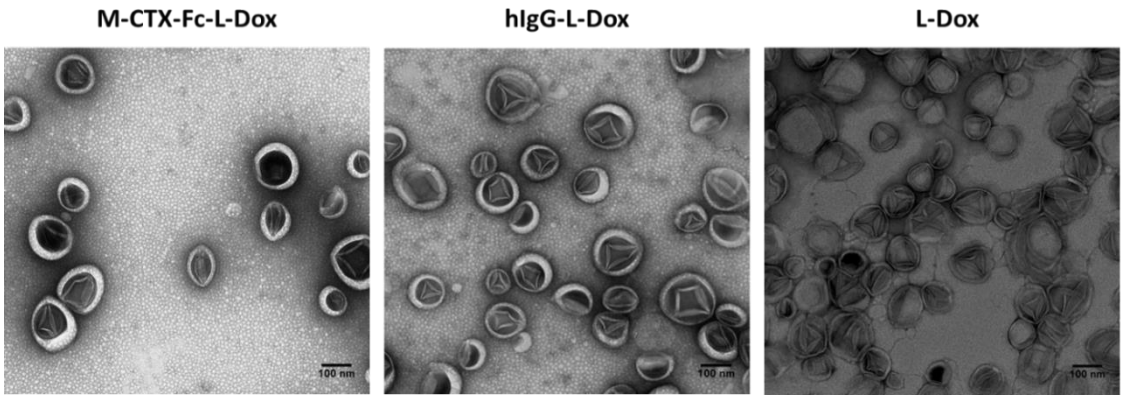

Figure 5: M-CTX-Fc-L-Dox showed unilamellar vesicles with diameter of approximately 100 nm. TEM images of liposome formulation encapsulating doxorubicin were compared between M-CTX-Fc-L-Dox, hIgG-L-Dox and L-Dox. Each scale bar shows 100nm**.**

3.5 Cellular uptake of liposomes

The cellular uptake of M-CTX-Fc-L-Dox and L-Dox into U251MG-P1 and SK-BR-3 cells was evaluated under a confocal microscope after 1 h incubation at 37°C (Figure 6). It is worth noting that the strong fluorescence of doxorubicin was observed in U251MG-P1 cells treated with M-CTX-Fc-L-Dox, especially in the nuclei. This observation might be attributed to the specific interaction of M-CTX-Fc-L-Dox with the cell surface molecule on U251MG-P1 cells by receptor-mediated endocytosis. On the other hand, when cells were treated with L-Dox, the fluorescence from L-Dox was reduced compared to that from M-CTX-Fc-L-Dox. It is important to mention that receptor-mediated

endocytosis achieved by M-CTX-Fc-L-Dox might be faster than the endocytosis gained by L-Dox only. This explanation agrees with our result for IT_{50} in figure 7. Oppositely, almost no signal for doxorubicin uptake was observed in the SK-BR-3 cells, which showed low expression of MMP-2 compared to U251MG-P1 cells. Collectively, M-CTX-Fc may have the potential to target MMP-2 expressing cancer cells and internalize into the cells while further investigation is required to identify the molecule on the cell surface directly binding to M-CTX-Fc.

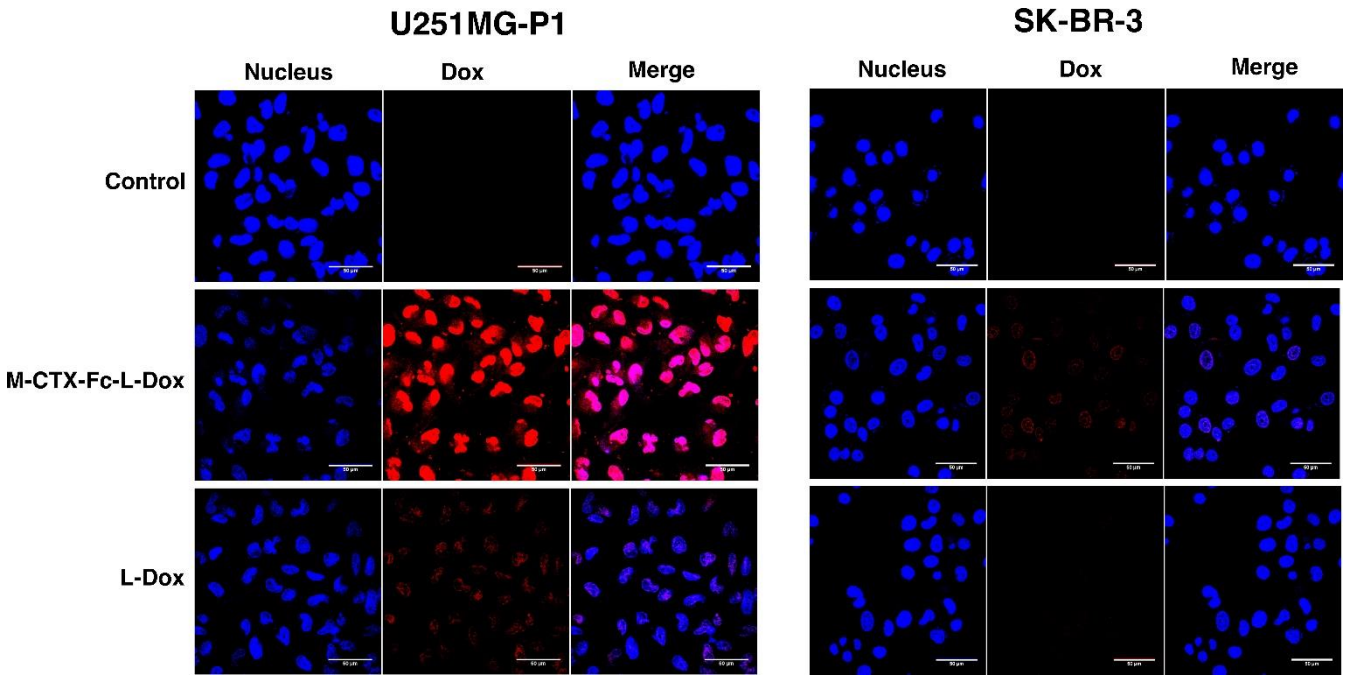

Figure 6. Cellular uptake of Doxorubicin in U251MG-P1 cells was enhanced through M-CTX-Fc-L-Dox. U251MG-P1 cells and SK-BR-3 cells were evaluated for the

cellular uptake of doxorubicin under a confocal microscope. Cell nuclei were stained with DAPI (blue). Red color arises from natural fluorescence properties of doxorubicin. Each scale bar shows 50 μm.

3.6 Cytotoxicity In Vitro

The IC_{50}s of doxorubicin were assessed when U251MG-P1 and SK-BR-3 cells were treated for 72 h with each formulation of naked doxorubicin, L-Dox, M-CTX-Fc-L-Dox and hIgG-L-Dox (**Figure 7**). Among the liposomal formulations, M-CTX-Fc-L-Dox showed the highest cytotoxicity with the lowest IC_{50} of 0.17 μM in U251MG-P1 cells. However, the cytotoxicity of M-CTX-Fc-L-Dox showed no significant different with naked doxorubicin. In SKBR-3 cells without MMP-2 expression, M-CTX-Fc-L-Dox appeared almost equally effective with hIgG-L-Dox and L-Dox. Collectively, the results appear consistent with the dependency of MMP-2 expression. As described previously, we thought the time of exposure allowing the cellular uptake should also be important to determine the effectiveness [22]. To make this point clearer, we evaluated the IT_{50}s.

In U251MG-P1 cells, M-CTX-Fc-L-Dox showed significantly rapid exposure time of IT_{50} at around 1.6 h. This is the shortest time when compared with those by other formulations. Meanwhile, in both cells, naked doxorubicin had rapid exposure time compared to L-Dox. This result could be explained by the difference of cellular mechanism of internalization. The cellular uptake of liposome is mediated by endocytosis, whereas the naked doxorubicin molecules internalized into the cell via passive diffusion. However, in the case of M-CTX-Fc-L-Dox, the conjugated ligand specific to MMP-2 receptor, exhibited shorter time for liposomes internalized into the cells and reaches IT50 comparable to the naked doxorubicin. On the other hand, in SK-BR-3 cells, no significant difference was found between L-Dox and M-CTX-Fc-L-Dox. Thus, M-CTX-Fc-L-Dox successfully demonstrated the specific targeting of U251MG-P1 cells *in vitro*.

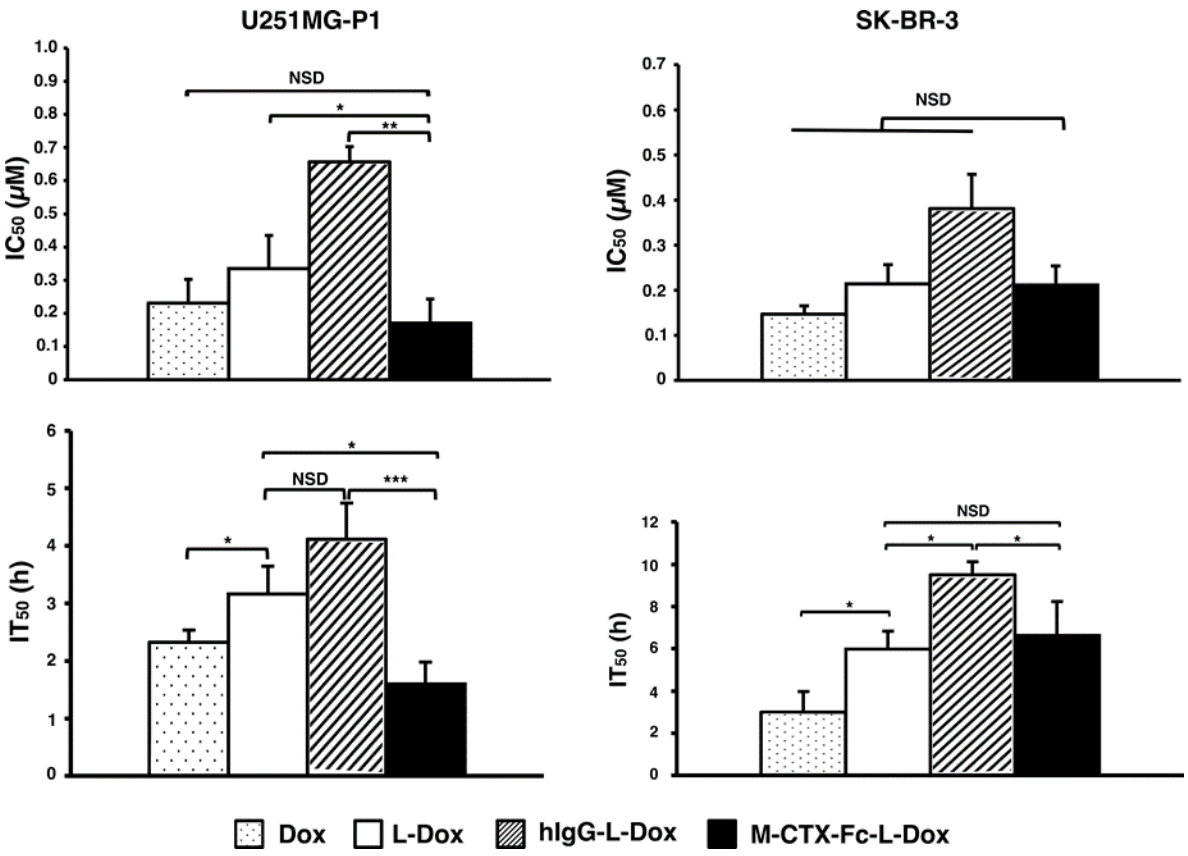

Figure 7: M-CTX-Fc-L-Dox exhibited the lowest inhibition concentration (IC_{50}) and shortest exposure time (IT_{50}) in U251MG-P1 cells. In vitro cytotoxicity IC_{50} of doxorubicin in different formulations after 72 h of exposure to U251MG-P1 and SK-BR-3 cells was evaluated and compared (top). IT_{50}s with doxorubicin at IC_{100} were evaluated and compared (bottom). The data presented as the mean ± S.D (n=3). The statistical significance in mean values of more than two groups was determined using one-way analysis of variance (ANOVA) and post hoc Tukey HSD were applied using M-CTX-Fc-L-Dox liposome as control. *, P<0.05; **, P<0.01; ***, P<0.005; ****, P<0.001. NSD, no significant difference. #, P<0.05 versus Dox.

3.7 Suppression of tumor growth *In Vivo*

The suppression of tumor growth by M-CTX-Fc-L-Dox was evaluated in BALB/c mice bearing tumors of transplanted U251MG-P1 cells (Figure 8). We found that the tumor latency of U251MG-P1 is so rapid that it should not be comparable with that of U251MG cells. Meanwhile, the tumor latency of U251MG is not stable. This means that the targeting effect of our liposomal formulation is difficult to be demonstrated on the tumors from U251MG cells. First of all, the effect of doxorubicin on the body weight was assessed by the three-time injections of 10 mg/kg (Figure 8A). As the result, the loss of body weight was less than 20 % even when the naked doxorubicin was injected. The liposomal formulations were less toxic than naked doxorubicin as they showed body weight loss less than 10 %. After three times of injection in seven-day intervals, the tumor growth was observed for 20 days, and the efficacy of the suppression of tumor growth was calculated as a relative tumor volume normalized to the initial tumor volume before the treatment. The tumor volume in the PBS group increased aggressively, whereas M-CTX-Fc-L-Dox slowed the tumor growth more significant than naked Dox and hIgG-L-Dox at day 20 ($p<0.001$) (Figure 8B). M-CTX-Fc-L-Dox appeared slightly more effective than L-Dox at day 20 ($p = 0.043<0.05$). The representative tumors excised from the mice treated with five different formulations at day 20 demonstrated tumor suppression effect of M-CTX-Fc-L-Dox (Figure 8C). In this context, M-CTX-Fc-Dox exhibited an inhibitory effect on tumor growth, which could be attributed to the combined action of the

passive targeting via the EPR effect and active targeting via receptor-mediated endocytosis. However, a larger cohort-evaluation is needed to confirm the effect of M-CTX-Fc-L-Dox more precisely

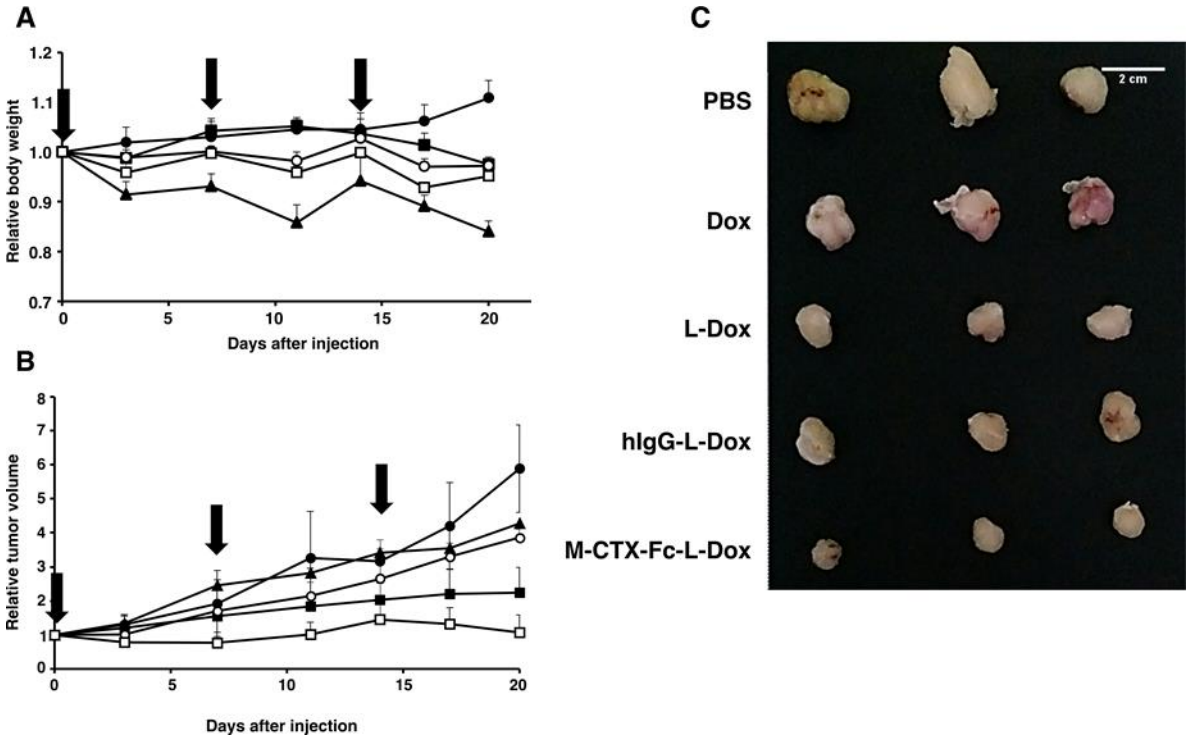

Figure 8: M-CTX-Fc-L-Dox suppressed tumor growth in the most effective manner in vivo. (A) The relative body weight of mice bearing tumors during the treatment. M-CTX-FC-L-Dox and other liposome formulations were less toxic than naked doxorubicin. The statistical significance in mean values of more than two groups was determined using one-way analysis of variance (ANOVA) and post hoc Tukey HSD were applied using relatives body weight of Dox treatment as control. ****, $P<0.001$. (B) The effect of different

formulations of doxorubicin on the volume of tumors. M-CTX-Fc-L-Dox was the most effective formulation to suppress the growth of tumor. Doxorubicin in each formulation was administered at 7- day intervals vertical arrows. The statistical significance in mean values of more than two groups was determined using one-way analysis of variance (ANOVA) and post hoc Tukey HSD were applied using relatives' tumor volume of M-CTX-Fc-L-Dox treatment as control, *, $P<0.05$; ****, $P<0.001$ (C) The tumors from the experiment (B) representing each group were displayed exhibiting the effect of each formulation of doxorubicin. Data are expressed as the mean with ±SD where n=3.

4.0 Conclusions

In our previous study, the U251MG-P1 cells has shown the CD44 expression was enriched when compared to the parental U251MG cells, along with aberrant activation of principal stemness marker genes OCT3/4. SOX2, KLF4 and Nanog and with less expression of glial fibrillary acidic protein . This mean U251MG-P1 cells consist of rather undifferentiated cells than the parental U251MG cells. Additionally, U251MG-P1 cells are highly tumorigenic exhibiting rapid tumor growth in vivo, when compared to U251MG cells. This high tumorigenicity enabled us to study the drug delivery in vivo.

Drug delivery targeting cancer cells derived from glioblastoma was successfully demonstrated *in vitro* and *in vivo* with chlorotoxin fused to human IgG Fc domain in this study. As the results, chlorotoxin fusion protein shortened the IT_{50} of doxorubicin encapsulated in liposomes *in vitro* and suppressed the growth of tumor in vivo when compared with the liposomes without chlorotoxin ligand. Although we could not show the direct binding of M-CTX-Fc to MMP-2, we could show significant difference in the relative tumor growth between the treatment with M-CTX-Fc-L-Dox and that with L-Dox at day 20 ($P< 0.05$) This difference appeared to depend on the expression of MMP-2 according to the previous report, which demonstrated the specific interaction of chlorotoxin and MMP-2 [10].Thus, the combination of doxorubicin and chlorotoxin is proposed in this paper as a successful candidate of liposomal DDS formulation to target possibly glioblastoma stem cells and derivative tumor.

5.0 Supplementary data

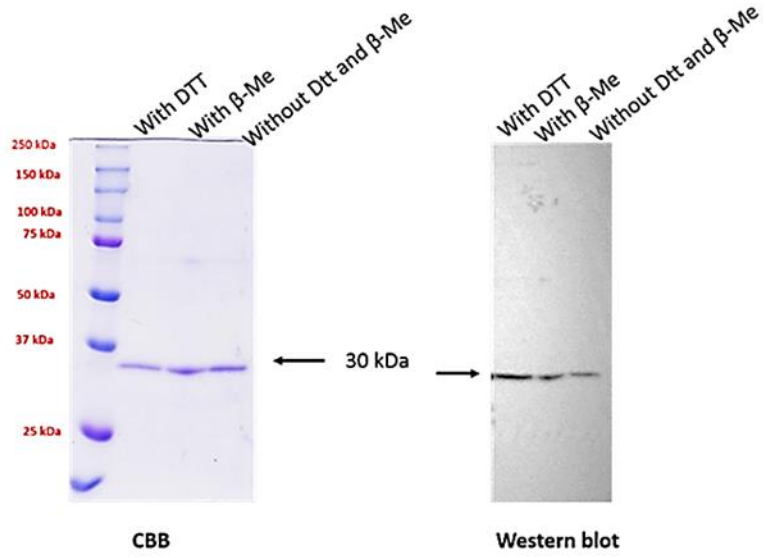

Figure S1. M-CTX-Fc in reducing and nonreducing conditions. Purified protein was subjected to SDS-PAGE and detected by CBB staining (left) and Western blotting with mouse monoclonal anti-human IgG antibody (right) as monomer at approximately 30 kDa.

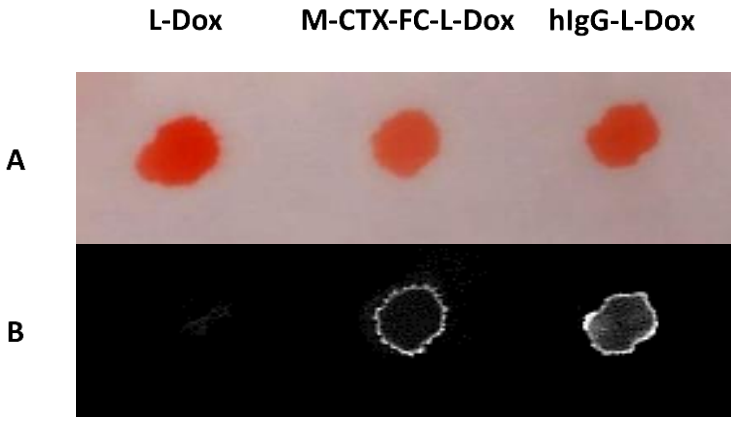

Figure S2. Dot blotting analysis of liposomes conjugated to ligands. Liposomes containing approximately 1 µg of doxorubicin in 3 µL were blotted onto PVDF membrane (A) and probed with mouse monoclonal anti-human IgG antibody conjugated with HRP (B). The immunoreactivity indicates the successful conjugation of M-CTX-Fc and hIgG to liposomes.

References

1. van Tellingen, O., et al., *Overcoming the blood–brain tumor barrier for effective glioblastoma treatment.* Drug Resistance Updates, 2015. **19**(Supplement C): p. 1-12.
2. Davis, M.E., *Glioblastoma: Overview of Disease and Treatment.* Clinical journal of oncology nursing, 2016. **20**(5): p. S2-S8.
3. Wang, S., et al., *Receptor-Mediated Drug Delivery Systems Targeting to Glioma.* Nanomaterials, 2016. **6**(1): p. 3.
4. Chen, J., et al., *A restricted cell population propagates glioblastoma growth following chemotherapy.* Nature, 2012. **488**(7412): p. 522-526.
5. Jhanwar-Uniyal, M., et al., *Glioblastoma: Molecular Pathways, Stem Cells and Therapeutic Targets.* Cancers, 2015. **7**(2): p. 538-555.
6. Ramachandran, R.K., et al., *Expression and prognostic impact of matrix metalloproteinase-2 (MMP-2) in astrocytomas.* PLoS ONE, 2017. **12**(2): p. e0172234.
7. Sato, H. and T. Takino, *Coordinate action of membrane-type matrix metalloproteinase-1 (MT1-MMP) and MMP-2 enhances pericellular proteolysis and invasion.* Cancer Science, 2010. **101**(4): p. 843-847.
8. Bauvois, B., *New facets of matrix metalloproteinases MMP-2 and MMP-9 as cell surface transducers: Outside-in signaling and relationship to tumor progression.*

Biochimica et Biophysica Acta (BBA) - Reviews on Cancer, 2012. **1825**(1): p. 29-36.

9. DeBin, J.A. and G.R. Strichartz, *Chloride channel inhibition by the venom of the scorpion Leiurus quinquestriatus.* Toxicon, 1991. **29**(11): p. 1403-1408.
10. Deshane, J., C.C. Garner, and H. Sontheimer, *Chlorotoxin Inhibits Glioma Cell Invasion via Matrix Metalloproteinase-2.* Journal of Biological Chemistry, 2003. **278**(6): p. 4135-4144.
11. Lyons, S.A., J. O'Neal, and H. Sontheimer, *Chlorotoxin, a scorpion-derived peptide, specifically binds to gliomas and tumors of neuroectodermal origin.* Glia, 2002. **39**(2): p. 162-173.
12. Graf, N., et al., *Platinum(IV)-chlorotoxin (CTX) conjugates for targeting cancer cells.* Journal of Inorganic Biochemistry, 2012. **110**(Supplement C): p. 58-63.
13. Fang, C., et al., *Temozolomide Nanoparticles for Targeted Glioblastoma Therapy.* ACS applied materials & interfaces, 2015. **7**(12): p. 6674-6682.
14. Soroceanu, L., et al., *Use of Chlorotoxin for Targeting of Primary Brain Tumors.* Cancer Research, 1998. **58**(21): p. 4871-4879.
15. Qin, C., et al., *The impact of a chlorotoxin-modified liposome system on receptor MMP-2 and the receptor-associated protein ClC-3.* Biomaterials, 2014. **35**(22): p. 5908-5920.

16. Kasai, T., et al., *Chlorotoxin Fused to IgG-Fc Inhibits Glioblastoma Cell Motility via Receptor-Mediated Endocytosis.* Journal of Drug Delivery, 2012. **2012**: p. 975763.

17. El-Ghlban, S., et al., *Chlorotoxin-Fc Fusion Inhibits Release of MMP-2 from Pancreatic Cancer Cells.* BioMed Research International, 2014. **2014**: p. 10.

18. Arun vaidyanath, H.B.M., Apriliana Cahya Khayrani, Aung KoKo Oo, Akimasa Seno, Mami Asakura, Tomonari Kasai and Masaharu Seno, *Hyaluronic Acid Mediated Enrichment of CD44 Expressing Glioblastoma Stem Cells in U251MG Xenograft Mouse Model.* Journal of Stem Cell Research & Therapy, 2017. **7**(4).

19. Abraham, S.A., et al., *The Liposomal Formulation of Doxorubicin*, in *Methods in Enzymology*. 2005, Academic Press. p. 71-97.

20. Alyane, M., G. Barratt, and M. Lahouel, *Remote loading of doxorubicin into liposomes by transmembrane pH gradient to reduce toxicity toward H9c2 cells.* Saudi Pharmaceutical Journal, 2016. **24**(2): p. 165-175.

21. Shigehiro, T., et al., *Evaluation of glycosylated docetaxel-encapsulated liposomes prepared by remote loading under solubility gradient.* Journal of Microencapsulation, 2016. **33**(2): p. 172-182.

22. Shigehiro, T., et al., *Efficient Drug Delivery of Paclitaxel Glycoside: A Novel Solubility Gradient Encapsulation into Liposomes Coupled with Immunoliposomes Preparation.* PLoS ONE, 2014. **9**(9): p. e107976.

23. Fabel, K., et al., *Long-term stabilization in patients with malignant glioma after treatment with liposomal doxorubicin.* Cancer, 2001. **92**(7): p. 1936-1942.

24. Hau, P., et al., *Pegylated liposomal doxorubicin-efficacy in patients with recurrent high-grade glioma.* Cancer, 2004. **100**(6): p. 1199-1207.

25. Fosgerau, K. and T. Hoffmann, *Peptide therapeutics: current status and future directions.* Drug Discovery Today, 2015. **20**(1): p. 122-128.

26. Czajkowsky, D.M., et al., *Fc-fusion proteins: new developments and future perspectives.* EMBO Molecular Medicine, 2012. **4**(10): p. 1015-1028.

27. Sekhar, S.C., et al., *Identification of Caveolin-1 as a Potential Causative Factor in the Generation of Trastuzumab Resistance in Breast Cancer Cells.* Journal of Cancer, 2013. **4**(5): p. 391-401.

28. Veiseh, M., et al., *Tumor Paint: A Chlorotoxin:Cy5.5 Bioconjugate for Intraoperative Visualization of Cancer Foci.* Cancer Research, 2007. **67**(14): p. 6882-6888.

29. Li, H., et al., *Effect of ligand density and PEG modification on octreotide-targeted liposome via somatostatin receptor in vitro and in vivo.* Drug Delivery, 2016. **23**(9): p. 3562-3572.

30. Chu, C., et al., *Effect of surface ligand density on cytotoxicity and pharmacokinetic profile of docetaxel loaded liposomes.* Asian Journal of Pharmaceutical Sciences, 2016. **11**(5): p. 655-661.

31. Düzgüneş, N. and S. Nir, *Mechanisms and kinetics of liposome–cell interactions.* Advanced Drug Delivery Reviews, 1999. **40**(1): p. 3-18.

32. Drummond, D.C., et al., *Optimizing Liposomes for Delivery of Chemotherapeutic Agents to Solid Tumors.* Pharmacological Reviews, 1999. **51**(4): p. 691-744.

LIST OF PUBLICATION

REFERRAL PAPER

1) Targeting Glioblastoma Cells Expressing CD44 with Liposomes Encapsulating Doxorubicin and Displaying Chlororotoxin IgG-Fc Fusion Protein.

   Hafizah Mahmud, Tomonari Kasai, Apriliana Cahya Khayrani , Mami Asakura , Aung Ko Ko Oo , Du Juan , Arun Vaidyanath , Samah El-Ghlban , Akifumi Mizutani, Akimasa Seno, Hiroshi Murakami, Junko Masuda and Masaharu Seno. International Journal of Molecular Sciences. 2018, 19: 659.

2) Hyaluronic Acid Mediated Enrichment of CD44 Expressing Glioblastoma Stem Cells in U251MG Xenograft Mouse Model

   Arun Vaidyanath, **Hafizah Mahmud**, Apriliana Cahya Khayrani, Aung KoKo Oo, Akimasa Seno, Mami Asakura, Tomonari Kasai and Masaharu Seno.Journal of Stem Cell Research & Therapy, 2017, 7: 384 (paper ID: 384)

ORAL OR POSTER PRESENTATION

1) Evaluation of Drug Delivery System Targeting Glioblastoma Cells using Liposome Modified with Monomeric Fusion Protein of Cholorotoxin (Poster presentation)

   Hafizah Mahmud, Tomonari Kasai, Apriliana Cahya Khayrani, Aung Ko Ko Oo, Masaharu Seno.The International Conferences and Exhibition on Nanomedicine and Drug Delivery, Vol 6, No. 4. (Osaka, 2017.05.30)

2) Liposome Conjugated with Monomeric Fusion Protein of Chlorotoxin (M-CTX-Fc) Targeting to Malignant Glioblastoma Cells (Poster presentation)

   Hafizah Mahmud, Tomonari Kasai, Apriliana Cahya Khayrani, Arun Vaidyanath, Aung Ko Ko Oo, Du Juan, Masaharu Seno. Consortium of Biological Sciences 2017, The Molecular Society of Japan, No 40th Annual Meeting (Kobe, 2017-12 7).

3) Delivery of Liposomal Paclitaxel Glycoside to Glioblastoma Cells Targeting CD44 (Poster Presentation)

   Apriliana Cahya Khayrani, Tomonari Kasai, **Hafizah Mahmud,** Tsukasa Shigehiro, Arun Vaidyanath, Aung Ko Ko Oo, Koji Hara, Hiroki Yamada, Yuhki Seno, Takadatsu Mandai, Du Juan, Masaharu Seno. Consortium of Biological

Sciences 2017, The Molecular Society of Japan, No 40th Annual Meeting (Kobe, 2017-12-7)

4) Analysis of the differential methylated regions in the cancer stem cell model converted from iPSCs. (Poster Presentation)
Aung Ko Ko Oo, Arun Vaidyanath, Anna Sanchez Calle, **Hafizah Mahmud**, Neha Nair, Apriliana Cahya Khayrani, Md Jahangir Alam, Tomonari Kasai, Masaharu Seno. Consortium of Biological Sciences 2017, The Molecular Society of Japan, No 40th Annual Meeting (Kobe, 2017-12-7).

5) Analysis of the Conversion of iPSCs into Cancer Stem Cells with Non-Mutagenic Chemical Compounds. (Poster Presentation)
Juan Du, Tomonari Kasai, Aung Ko Ko Oo, Saki Sasada, Apriliana Cahya Khayrani, **Hafizah Mahmud**, Neha Nair, Arun Vaidyanath, Masaharu Seno. Consortium of Biological Sciences 2017, The Molecular Society of Japan, No 40th Annual Meeting (Kobe, 2017-12-7).

6) Targeting of glioblastoma with multivalent of anti-CD44 antibody-paclitaxel glycoside liposome. (Poster presentation)
Apriliana Cahya Khayrani, Tomonari Kasai , **Hafizah Mahmud**, Tsukasa Shigehiro, Arun Vaidyanath, Aung Ko Ko Oo, Masaharu Seno.

The International Conferences and Exhibition on Nanomedicine and Drug Delivery Vol 6, No. 4. (Osaka, 2017.05.30).

7) iPSC derived CSC model with lung metastasis developed in the microenvironment of lung carcinoma. (Poster presentation)

Aung Ko Ko Oo, Tomonari Kasai, Arun Vaidyanath, **Hafizah Mahmud**, Neha Nair, Anna Sanchez Calle, Masaharu Seno.The American Society for Cell Biology, Annual meeting 2016. (San Francisco California, 2016.12.6)